

## Two new Geoplaninae species (Platyhelminthes: Continenticola) from Southern Brazil based on an integrative taxonomic approach

Ilana Rossi<sup>a,b</sup>, Silvana Vargas Amaral<sup>a,b</sup>, Giovana Gamino Ribeiro<sup>c</sup>,  
Guilherme Pinto Cauduro<sup>b,c</sup>, Israel Fick<sup>a,b</sup>, Victor Hugo Valiati<sup>b,c</sup>  
and Ana Maria Leal-Zanchet <sup>a,b</sup>

<sup>a</sup>Instituto de Pesquisas de Planárias, Universidade do Vale do Rio dos Sinos – UNISINOS, São Leopoldo, Brazil; <sup>b</sup>Programa de Pós-Graduação em Biologia, Universidade do Vale do Rio dos Sinos – UNISINOS, São Leopoldo, Brazil; <sup>c</sup>Laboratório de Biologia Molecular, Universidade do Vale do Rio dos Sinos – UNISINOS, São Leopoldo, Brazil

### ABSTRACT

The genera *Cratera* Carbayo *et al.*, 2013 and *Obama* Carbayo *et al.*, 2013, belonging to the subfamily Geoplaninae, were recently proposed to encompass some of the species that belonged to the genus *Geoplana* Stimpson, 1857. Herein we describe two new species of Geoplaninae, occurring in areas of ombrophilous forest which belong to the southern portion of the Brazilian Atlantic Rain Forest. The species are sympatric in their type-locality. In general, both new species herein described match the diagnostic characteristics of their genera. However, some of these features are noteworthy when characters of the new species are taken into consideration, especially the pattern of the sensory pits and the morphology of the prostatic vesicle. Both species are differentiated from their congeners by a combination of morphological characteristics, corroborated by phylogenetic analyses of the cytochrome *c* oxidase subunit I gene, using maximum likelihood and Bayesian inference, as well as the Automatic Barcode Gap tool.

### ARTICLE HISTORY

Received 14 May 2015  
Accepted 31 July 2015  
Online 29 October 2015

### KEYWORDS

Integrative taxonomy; land planarians; triclads; Neotropical region; ombrophilous forest; Atlantic Forest

## Introduction

The subfamily Geoplaninae, the distribution of which is restricted to the Neotropical region, is currently composed of 24 genera (Sluys *et al.* 2009; Carbayo 2010; Grau *et al.* 2012; Carbayo *et al.* 2013). Among them, the genera *Cratera* Carbayo *et al.*, 2013 and *Obama* Carbayo *et al.*, 2013 were recently proposed to encompass some of the species that belonged to the genus *Geoplana* Stimpson, 1857. This proposal was based on molecular analyses and supported by morphological data (Carbayo *et al.* 2013).

Currently, the genera *Cratera* and *Obama* include 8 and 36 known species, respectively, most of them recorded for areas covered by dense ombrophilous forest, in the Brazilian

**CONTACT** Ana Maria Leal-Zanchet  [zanchet@unisinis.br](mailto:zanchet@unisinis.br)

<http://www.zoobank.org/urn:lsid:zoobank.org:pub:27E39852-A9E3-404D-B402-70DFAB21B361>

 Supplemental material for this article can be accessed here.

© 2015 Taylor & Francis

state of São Paulo (Carbayo and Froehlich 2008; Amaral et al. 2012; Rossi et al. 2014; Álvares-Presas et al. 2015; Carbayo and Almeida 2015). A high species diversity of land flatworms has been recorded in the southern portions of the Brazilian Atlantic Rain Forest, in areas covered by mixed ombrophilous forest (with *Araucaria angustifolia*), but most of them are still undescribed (Leal-Zanchet and Baptista 2009; Leal-Zanchet et al. 2011).

In spite of the existence of some works that use morphological and molecular methods to delimit new species of land planarians (Mateos et al. 1998; Jones et al. 2008; Lemos et al. 2014; Álvares-Presas et al. 2015), most taxonomical descriptions are exclusively based on morphological studies. Herein we describe, through an integrative methodology, two new species of land flatworms occurring in areas covered by ombrophilous forest, which are sympatric in their type-locality.

## Material and methods

The type-locality of both new species and the two other sampling localities are located on the eastern border of the Araucaria Plateau, in southern Brazil. The type-locality, the National Forest of São Francisco de Paula (29°23' to 29°27'S, 50°23' to 50°25'W), with altitudes ranging from 600 to 960 m above sea level (a.s.l.), was originally dominated by mixed ombrophilous forest and natural grasslands. Nowadays, remnants of this type of forest form a heterogeneous mosaic landscape mixed with old-tree monocultures of *Araucaria angustifolia* (Bertol.) O. Kuntze, *Pinus* and *Eucalyptus*. The Research and Conservation Center Pró-Mata (29°28' to 29°31'S, 50°08' to 50°14'W) is a private area mainly covered by fragments of Araucaria Forest immersed in a matrix of natural grasslands at high altitudes (900 m a.s.l.), and by continuous dense ombrophilous forest at lower altitudes (600 m a.s.l.). The National Park of Aparados da Serra (29°05' to 29°15'S, 50°00' to 50°15'W) encompasses two main types of forest, mixed ombrophilous forest, which occurs in fragments surrounded by dry and wet grassland at an altitude of approximately 900 m, and a continuous area of dense ombrophilous forest located at around 40 m a.s.l. (Leal-Zanchet et al. 2011). The regional climate is subtropical and humid, without extreme dry periods (Nimer 1989), and with an annual rainfall between 1750 and 2500 mm/year (IBGE 1986). The mean annual temperature is less than 16°C (IBGE 1986).

Specimens of both new species were collected during the day by direct sampling in leaf litter, under and inside fallen logs and under stones. The specimens collected, locality data, and identification and GenBank accession numbers are listed in Supplementary material, Table S1 and in their respective sections of the taxonomic account presented below.

## Morphological analysis

Live specimens were analysed regarding colour pattern and body shape and dimensions. Before fixation, the posterior tip of eight specimens was cut and fixed in 100% ethyl alcohol for molecular analysis. After that, specimens were killed with boiling water and fixed in neutral formalin 10% and subsequently maintained in 70% ethyl alcohol. Characteristics of the external morphology, such as colour pattern, body length and width, mouth and gonopore position and distribution of eyes, were analysed under a stereomicroscope. The analyses of eye distribution was also done after immersing fixed specimens in clove oil for 4 days.

Body fragments, namely the anterior tip, the subsequent body region containing ovaries, a pre-pharyngeal region and the body regions containing the pharynx and the copulatory apparatus, were cut, dehydrated in an ascending ethyl alcohol series, cleared in isopropyl alcohol and embedded in Paraplast®. Histological sections made at intervals of 6 µm were stained with haematoxylin & eosin or Goldner's Masson trichrome (Romeis 1989).

The ratio of the height of the cutaneous musculature to the height of the body (mc : h index in C. G. Froehlich 1955) was determined in the median region of a transverse section of the pre-pharyngeal region. Mesenchymal muscle fibres were counted in transverse sections of the same region. Colour descriptors, based on the uptake of dyes of particular colours, were used for classifying secretions with trichrome methods: erythrophil, xanthophil and cyanophil.

Type-material was deposited in the Museu de Zoologia da Universidade do Vale do Rio dos Sinos, São Leopoldo, Rio Grande do Sul, Brazil (MZU), and the Helminthological Collection of Museu de Zoologia da Universidade de São Paulo, São Paulo, São Paulo State, Brazil (MZUSP).

### **Nucleic acid isolation and sequence analysis**

DNA isolation, polymerase chain reaction (PCR) amplification and sequencing of amplicons' DNA were performed from five specimens of *Obama maculipunctata* sp. nov. and three of *Cratera ochra* sp. nov., preserved in 100% ethanol (see Supplementary material, Table S1) using the Wizard® Genomic DNA Purification Kit (Promega, Madison, WI, USA) according to the manufacturer's instructions. The following primers were used to amplify a region of the cytochrome c oxidase subunit I (COI): BarT (5'-ATG ACD GCS CAT GGT TTA ATA ATG AT-3') (Álvarez-Presas et al. 2011); COIR (5'-CCW GTY ARM CCH CCW AYA GTA AA-3') (Lázaro et al. 2009), FlatwormCOI (5'-GCAGTTTTGGTTTTGGACATCC-3') and FlatwormCOIR (5'-GAGCAACAACATAATAAGTATCATG-3') (Sunnucks et al. 2006). The same primers were used for sequencing. The PCR amplification for COI was carried out in a total volume of 25 µl including 20–50 ng of genomic DNA, 0.2 µM of each primer, 200 µM dNTPs, 1 × buffer, 1.5 mM MgCl<sub>2</sub>, 1 unit of *Taq* DNA polymerase (Invitrogen, Carlsbad, CA, USA) and ultrapure H<sub>2</sub>O. The conditions for amplifying the COI mitochondrial gene were 95°C for 3 min (denaturation), 38 cycles of 50 sec at 94°C (denaturation), 60 sec at 50°C (annealing) and 50 sec at 72°C (extension), then 72°C for 5 min. The PCR results were verified through electrophoresis of the amplicons on 1% agarose gels stained with GelRed (Biotium, Hayward, CA, USA), and visualized under UV transillumination. PCR products were purified using Shrimp Alkaline Phosphatase and exonuclease I (New England Biolabs, Ipswich, MA, USA) following the manufacturer's recommendations. Amplicons were submitted to direct sequencing at Macrogen (Macrogen Inc., Seoul, Korea), and each sample was sequenced in both directions.

### **Sequence and phylogenetic analysis**

Quality of sequences was evaluated using ChromasPro 1.5 software (<http://www.techne.lysium.com.au>). Sequences were then aligned within ClustalW 2.1 (Thompson et al. 1997), inspected manually using Bioedit 7.1.3 (Hall 1999) to refine coding frame and checked using the BLASTn on-line tool for comparison with sequences deposited in the GenBank database (NCBI). The amino acid translation was examined to ensure that no gaps or stop codons were present in the alignment. Two phylogenetic analyses were

performed on all data sets, a maximum likelihood analysis using RAxML 7.2.8 (Stamatakis et al. 2008) and Bayesian inference of phylogeny performed with MrBayes (Ronquist and Huelsenbeck 2003). The optimum substitution models were first determined by the programs Modeltest (Posada and Crandall 1998) and PAUP (Swofford 1998). The Akaike information criterion results from Modeltest provided the GTR + I + G model as the best fit for the substitution model. The Bayesian inference of phylogeny, performed with default priors and three heated and one cold Markov chains, was run from two random starting points. The Markov chain Monte Carlo search was run with 50,000,000 generations (repeated twice), sampled at every 1000 generations; the first 25% trees were discarded as 'burn-in,' after which the chain reached a stationary state, which ensured that the average split frequencies between the runs was < 1%. In addition, pairwise nucleotide distances between all sequences were calculated according to Kimura's two-parameter model and 1000 bootstraps (Kimura 1980) using MEGA version 5.1 (Tamura et al. 2011). The Automatic Barcode Gap (ABGD) tool (Puillandre et al. 2012) was employed to verify the distribution of genetic pairwise distances and potential barcoding gaps. COI distance matrices produced by MEGA were uploaded to <http://www.wabi.snv.jussieu.fr/public/abgd/abgdweb.html>. ABGD was run with default settings ( $P_{\min} = 0.001$ ,  $P_{\max} = 0.1$ , Steps = 10, X [relative gap width] = 15, Nb bins = 20, and with Kimura two-parameter distances).

### Abbreviations used in the figures

The following abbreviations are used in the figures: cg, cyanophil glands; cmc, common muscle coat; cov, common glandular ovovitelline duct; db, dorsal bands; de, dorsal epidermis; di, dorsal insertion; dm, dorsal cutaneous musculature; e, eyes; eg, erythrophil glands; ej, ejaculatory duct; es, oesophagus; fa, female atrium; fc, female canal; gm, glandular margin; go, gonopore; i, intestine; im, internal musculature; lu, pharyngeal lumen; lf, lateral flecks; m, mouth; ma, male atrium; me, monolobated eyes; mf, median flecks; mg, mixed glands; mm, mesenchymal musculature; ms, median spots; n, nerve cord; o, ovary; om, outer musculature; ov, ovovitelline duct; p, penis papilla; pma, para-marginal stripes; pp, pharyngeal pouch; pv, prostatic vesicle; sg, shell glands; sp, sensory pit; sv, spermiducal vesicle; t, testes; te, trilobated eyes; v, vitellaria; ve, ventral epidermis; vi, ventral insertion; vm, ventral cutaneous musculature; xg, xanthophil glands.

## Results

### Molecular results

The two phylogenetic methods used in the present study (maximum likelihood and Bayesian inference) revealed similar topologies and indicated that the two species herein studied belong to the genera *Cratera* and *Obama*, respectively (Figure 1). The phylogenetic analyses also indicated that both species are clearly delimited from their congeners (Figure 1) and, hence, they are herein described as new species. Among pairwise combination of 33 specimens of various species of the genera *Cratera* and *Obama*, as well as of *Pasipha* as an out group, the mean COI gene divergence was 13.2% with a range of 0–19.6%. Measures of intraspecific and interspecific variation of the COI gene indicated that the genetic divergence of species of these genera ranged from 0% to 1.4% (*Pasipha*), 0.3% to 2.8% (*Obama*) and 0% to 0.3% (*Cratera*) (mean = 0.6%) for

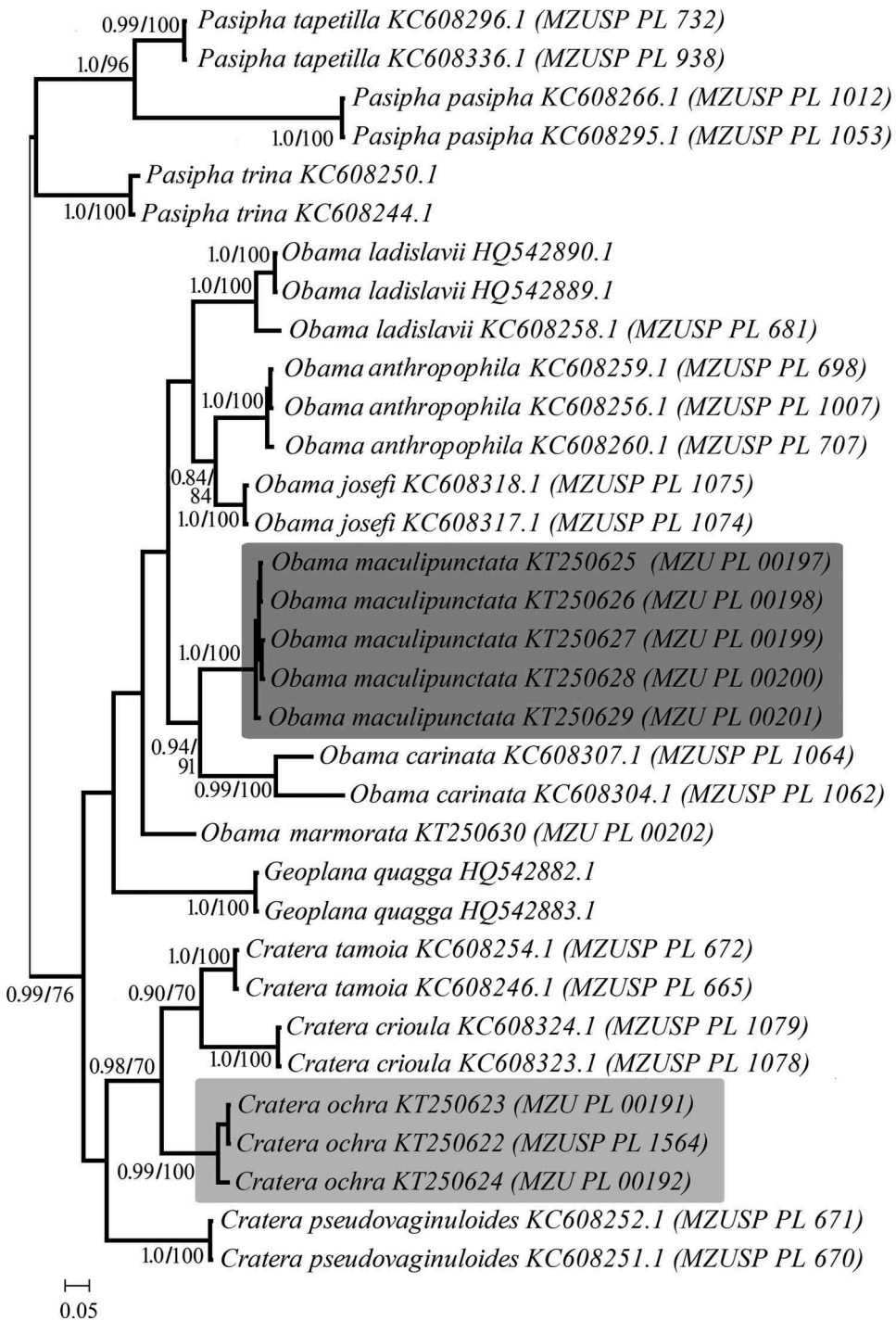


**Figure 1.** Bayesian phylogenetic tree inferred from the 640-bp of cytochrome c oxidase subunit I gene under GTR + I + G model of sequence evolution. The two new species are highlighted in light grey (*Cratera ochra* sp. nov.) and dark grey (*Obama maculipunctata* sp. nov.). Values indicate support for each node according to the maximum posterior probabilities >70% and bootstrap support values > 70%, respectively.

intraspecific comparisons and from 10.2% to 13% (mean = 11.7%) for congeneric comparisons, much lower than the mean interspecific divergence. An exception was found for the species *Obama carinata* ( $8.6 \pm 1.2\%$ ), whose intraspecific distances were higher than for the other species. Likewise, the results for the barcode gap thresholds obtained by ABGD show a distinct disjunction between what is presumed to be intraspecific variation (< 3%) and interspecific divergence (> 5%).

## Taxonomy

Order **TRICLADIDA** Lang, 1884

Suborder **CONTINENTICOLA** Carranza et al., 1998

Family **GEOPLANIDAE** Stimpson, 1857

Subfamily **GEOPLANINAE** Stimpson, 1857

Genus *Cratera* Carbayo et al., 2013

*Cratera ochra* sp. nov.

(Figures 2–7)

Geoplanidae 4: Leal-Zanchet & Carbayo, 2000

Geoplanidae 2: Carbayo et al., 2002

*Geoplana* sp. 4: Leal-Zanchet & Baptista, 2009

*Geoplana* sp. 4: Leal-Zanchet et al., 2011

## Etymology

The specific name refers to the dorsal pigmentation, which is yellow-ochre.

## Type-material

**Holotype.** **MZUSP PL. 1564:** leg. P. K. Boll, 1 August 2013, São Francisco de Paula (National Forest of São Francisco de Paula), RS, Brazil – anterior tip: transverse sections on 21 slides; anterior region at the level of the ovaries: sagittal sections on 52 slides; pre-pharyngeal region: transverse sections on nine slides; pharynx: sagittal sections on 34 slides; copulatory apparatus: sagittal sections on 26 slides.

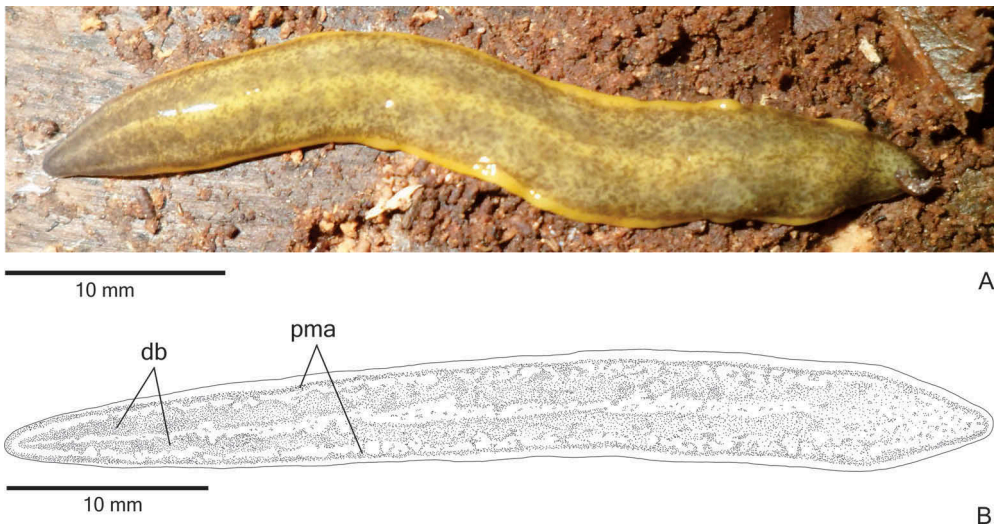


**Figure 2.** *Cratera ochra* sp. nov., holotype, in dorsal view. (A) Photograph of the live specimen. (B) Dorsal pattern of pigmentation of the preserved specimen.

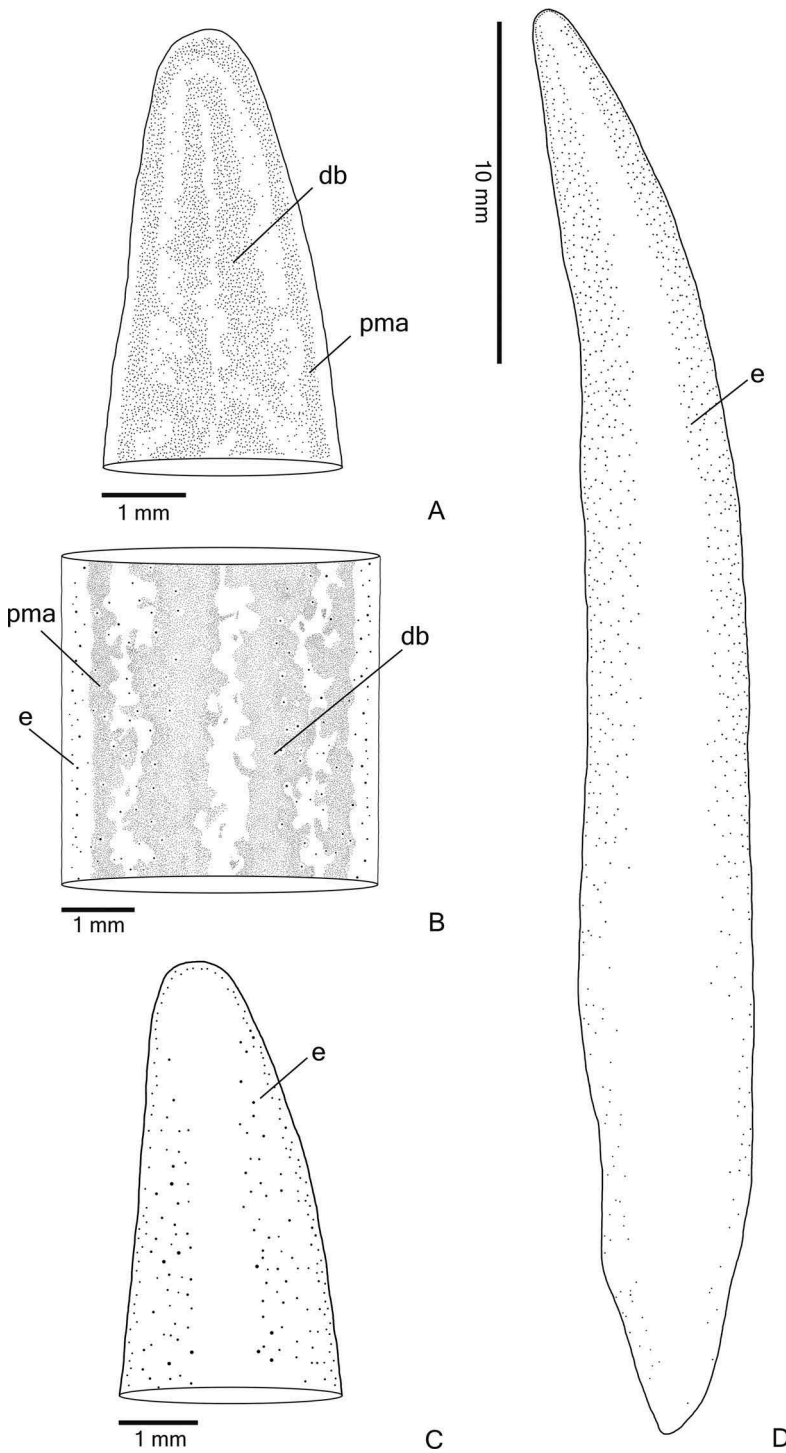


**Figure 3.** *Cratera ochra* sp. nov. in dorsal view. (A) Detail of the anterior extremity of the holotype. (B) Detail of the median third of the body of the holotype. (C) Detail of eye pattern at the anterior extremity of the holotype. (D) Eye pattern of a fixed specimen (paratype MZU PL.00187).

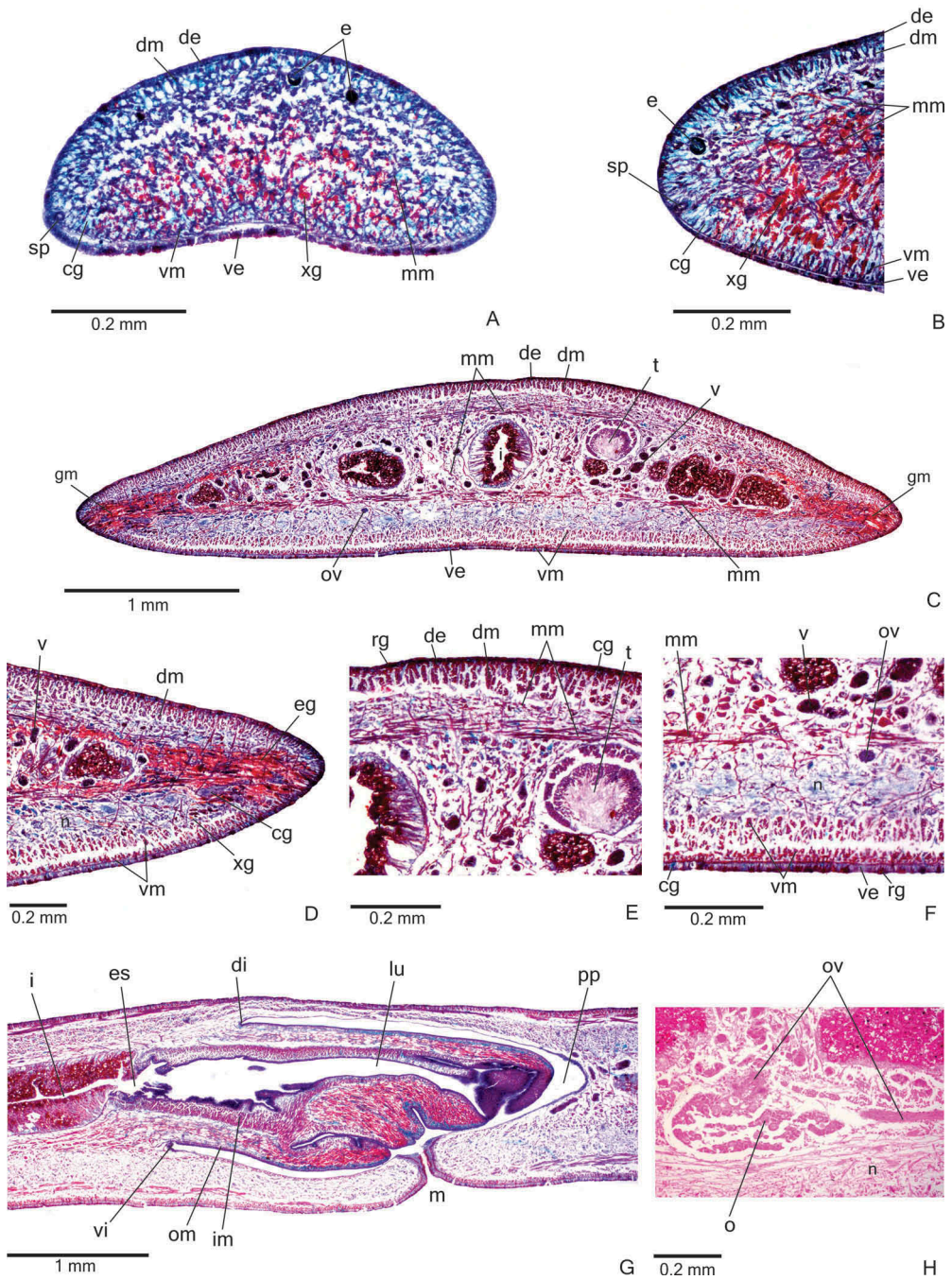


**Figure 4.** *Cratera ochra* sp. nov., holotype, in transverse (A–F) or sagittal (G, H) sections. (A) Anterior region of the body. (B) Detail of the anterior region of the body. (C) Pre-pharyngeal region. (D) Detail of body margin of the pre-pharyngeal region. (E) Detail of a dorsal portion of the pre-pharyngeal region. (F) Detail of a ventral portion of the pre-pharyngeal region. (G) Pharynx. (H) Ovary.

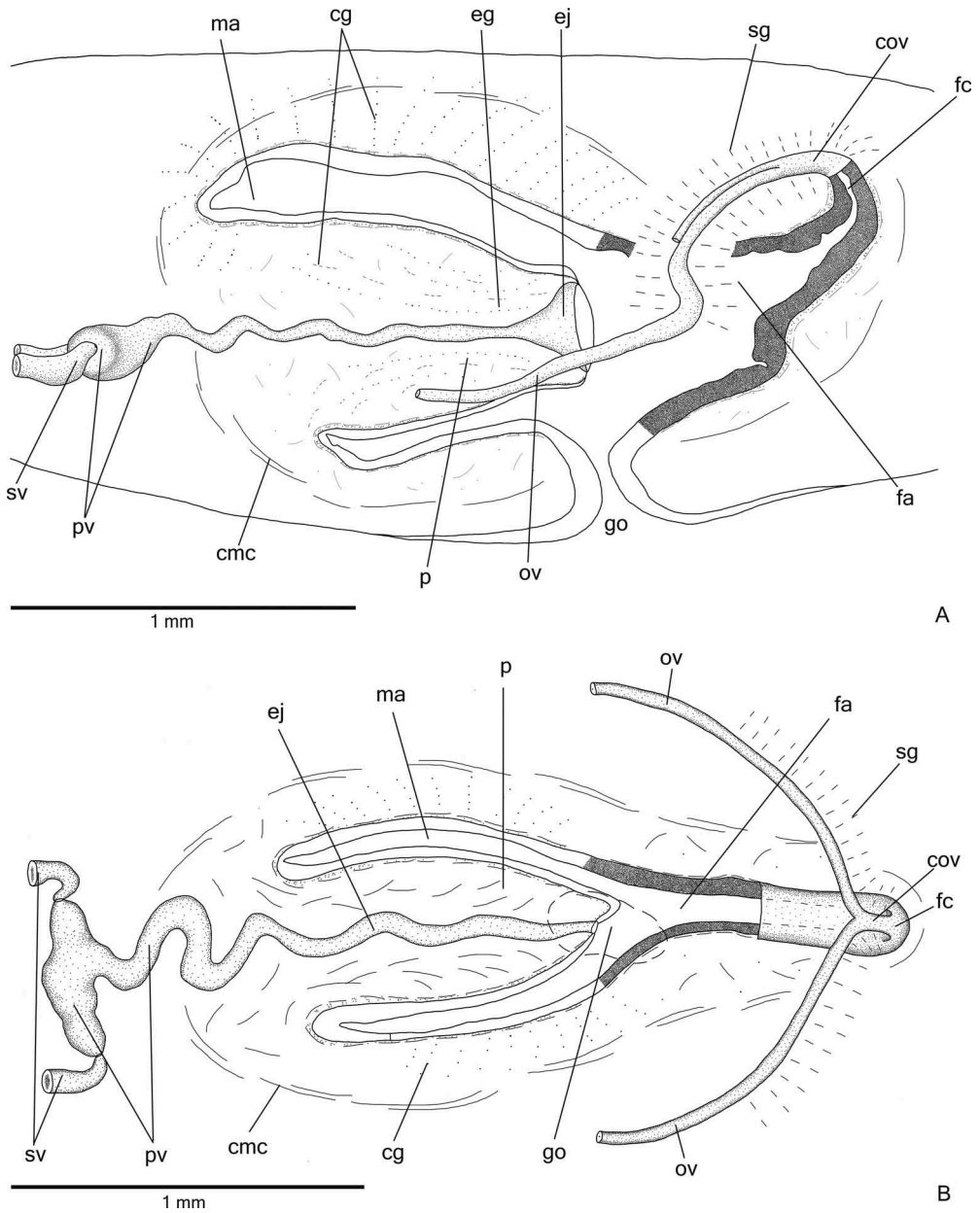


**Figure 5.** *Cratera ochra* sp. nov. (A) Sagittal composite reconstruction of the copulatory apparatus of the holotype. (B) Diagrammatic horizontal composite reconstruction of the copulatory apparatus of paratype MZU PL.00189.

**Paratypes.** São Francisco de Paula, RS, Brazil – **MZU PL.00187:** leg. R. Murowaniecki, 4 May 1998, National Forest of São Francisco de Paula – copulatory apparatus: sagittal sections on 26 slides; **MZU PL.00188:** leg. F. Carbayo, 8 June 1998, National Forest of São Francisco de Paula – anterior tip: transverse sections on 22 slides; region at the level of the ovaries: sagittal sections on 67 slides; pre-pharyngeal region: transverse sections on

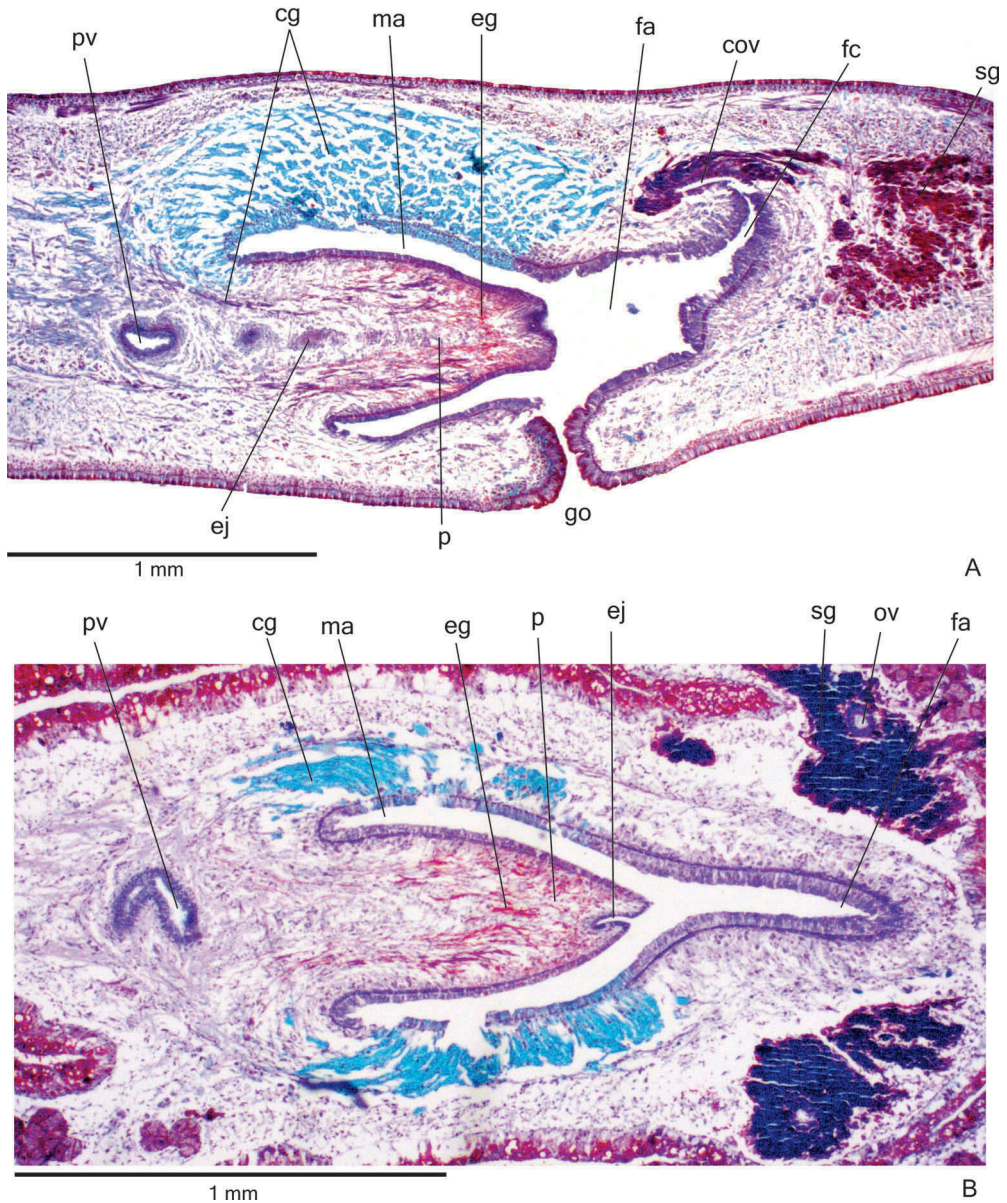


**Figure 6.** *Cratera ochra* sp. nov. (A) Copulatory apparatus of the holotype in sagittal section. (B) Copulatory apparatus of paratype MZU PL.00189 in horizontal section.

eight slides; pharynx: sagittal sections on 24 slides; copulatory apparatus: sagittal sections on 22 slides; **MZU PL.00189**: leg. F. Carbayo, 25 September 1998, National Forest of São Francisco de Paula – copulatory apparatus: horizontal sections on 22 slides; **MZU PL.00190**: leg. C. Palácios 17 October 2004, Research and Conservation Center Pró-Mata – pre-pharyngeal region: transverse sections on seven slides; pharynx: sagittal sections on 15 slides; copulatory apparatus: sagittal sections on 12 slides.

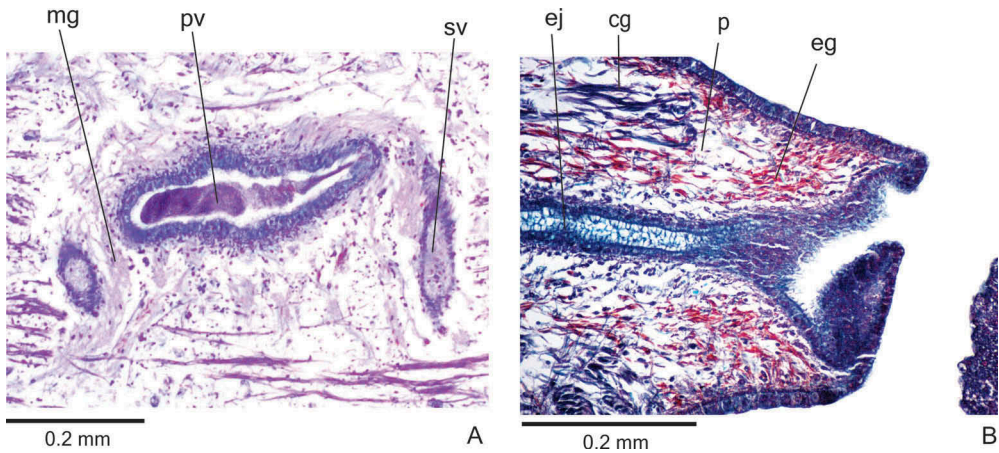


**Figure 7.** *Cratera ochra* sp. nov. (A) Detail of prostatic vesicle of paratype MZU PL.00189 in horizontal section. (B) Detail of tip of the penis papilla of the holotype in sagittal section.

### Diagnosis

Specimens of *Cratera* with yellow-ochre dorsal colour mainly with dispersed greyish or greyish-brown pigmentation constituting two broad dorsal bands; eyes dorsal; glandular margin with at least four types of glands; mc : h, 11–12%; pharynx cylindrical; prostatic vesicle extrabulbar with proximal portion ample and laterally expanded and distal portion tubular; ovovitelline ducts emerging dorsally from the median third of ovaries and ascending anterior to the gonopore.

**Molecular diagnosis.** This species includes all populations that cluster with specimens KT250622 to KT250624 (see Supplementary material, Table S1), with significant support in phylogenetic analyses.

### Type-locality

São Francisco de Paula (National Forest of São Francisco de Paula), state of Rio Grande do Sul (RS), Brazil.

### Distribution

Rio Grande do Sul (São Francisco de Paula), Brazil.

### Description

**External features.** Body broad with parallel margins and dorsal surface convex; anterior tip rounded and posterior tip pointed (Figure 2A). When creeping, maximum length reaches 85 mm. After fixation, maximum length was 52 mm (Table 1). Mouth and gonopore located at the posterior third of the body (Table 1).

In living animals, dorsal surface with dispersed greyish or greyish-brown pigmentation constituting two broad dorsal bands; the dorsal yellow-ochre ground colour is mainly visible between the dorsal bands and on the body margins. The ground colour is darker on the body margins than on the rest of the dorsal surface. The dorsal pigmentation concentrates at the anterior extremity (Figure 2A). Under the

**Table 1.** Measurements, in mm, of specimens of *Cratera ochra* sp. nov.

	Holotype MZUSP PL.1564	Paratype MZU PL.00187	Paratype MZU PL.00188	Paratype MZU PL.00189	Paratype MZU PL.00190
Maximum length in extension	54	–	70	72	40
Maximum width in extension	4.5	–	–	4	3
Length at rest	19	–	34	45	30
Width at rest	8	–	7	6	3
Length*	52	44	54	53	36
Width*	5	5	6.5	5.5	4
DM*	38 (73)	33 (75)	42 (78)	39 (73.5)	26 (72)
DG*	46 (88.5)	39 (88.5)	47 (87)	47 (88.5)	33 (91.5)
DMG*	8	6	5	8	7
DPVP	4.2	–	5.5	–	1.2
Ovaries	13.5 (26)	–	12 (22)	–	–
Anteriormost testes	15 (29)	–	16 (39.5)	–	–
Posteriormost testes	34.5 (66)	–	30 (55.5)	–	22.5 (62.5)
Prostatic vesicle	0.3	0.5	0.5	0.7	0.2
Penis papilla	1.1	0.6	1	0.9	0.4
Male atrium	1.1	0.7	1.3	0.95	0.5
Female atrium	0.8	0.2	0.5	0.8	0.2

–, not measured; \*, after fixation; DG, distance of gonopore from anterior end; DM, distance of mouth from anterior end; DMG, distance between mouth and gonopore; DPVP, distance between prostatic vesicle and pharyngeal pouch. The numbers given in parentheses represent the position relative to body length.

stereomicroscope, a greyish pigmentation forms two densely pigmented dorsal bands, as well as contours the anterior tip (Figures 2B, 3A). Posterior to the anterior tip, this pigmentation becomes more irregular and loosely arranged in flecks over the dorsum, making the yellow-ochre ground colour visible (Figures 2B, 3B). These flecks form the dorsal bands as well as paramarginal stripes. The dorsal bands become inconspicuous towards the posterior tip, where the pigmentation is more irregularly distributed (Figure 3B). Ventral surface pale yellow. After fixation, the dorsal pigmentation becomes greyish and mainly greyish-brown next to the margins; dorsal ground colour becomes pale yellow, as well as the ventral surface of the body.

Eyes monolobated. They are initially uniserial, with pigment cups of about 15  $\mu\text{m}$  in diameter, surrounding anterior tip (Figure 3C). After the second millimetre, the monolobated eyes become larger (with pigment cups of about 30  $\mu\text{m}$  in diameter) and spread onto the dorsal surface, occupying the maximum width of about 40% of the body width on each side of the body. Eyes remain dorsal, but become less numerous towards posterior tip (Figure 3D). Inconspicuous clear halos may occur around dorsal eyes (Figure 3B).

**Sensory organs, epidermis and body musculature.** Sensory pits (Figure 4A, B), as simple invaginations, contour anterior tip and occur ventromarginally in an irregular, single row in the anterior eighth of the body. Initially they occur at intervals of approximately 18  $\mu\text{m}$ , becoming gradually sparser. Their depth is about 25–50  $\mu\text{m}$ .

Creeping sole occupying the whole body width. Two types of glands discharge through dorsal epidermis and body margins of the pre-pharyngeal region: numerous rhabditogen cells with xanthophil secretion (rhammites) and cells with amorphous, cyanophil secretion (Figure 4E). Creeping sole receives the secretion from amorphous, cyanophil glands, as well as few rhabditogen cells with small, xanthophil rhabdites and cells with coarse granular, xanthophil secretion (Figure 4F). The glandular margin

**Table 2.** Body height and cutaneous musculature in the median region of a transverse section of the pre-pharyngeal region, in micrometers, and ratio of the height of cutaneous musculature to the height of the body (mc : h index) of specimens of *Cratera ochra* sp. nov.

	Holotype MZUSP PL.1564	Paratype MZU PL.00188	Paratype MZU PL.00190
Dorsal musculature	56	71	40
Ventral musculature	65	108	50
Body height	992	1500	806
mc : h (%)	12	12	11

(Figure 4C, D), which is visible after the second millimetre of the body, receives openings of at least four types of glands. Two of them are more numerous: glands with erythrophil, coarse granules, and glands with xanthophil, coarse granules. Other two types are scarcer: cyanophil glands with amorphous secretion and erythrophil glands with fine granules. On anterior tip, glands with cyanophil, amorphous secretion and rhabditogen glands with xanthophil secretion open through the whole surface of the body and glands with coarse granular, xanthophil secretion have numerous openings through the ventral epidermis (Figure 4A).

Cutaneous musculature with the usual three layers (circular, oblique and longitudinal layers), longitudinal layer with thick bundles (Figure 4C–F, Table 2). Cutaneous musculature thinner in the pre-pharyngeal region than in the anterior region of the body, gradually diminishing its thickness towards anterior tip (Figure 4A). Musculature becoming progressively lower towards body margins. Ventral musculature slightly higher than dorsal at the sagittal plane. Ratio of mc : h 11–12% (Table 2).

Mesenchymal musculature (Figure 4C, E, F) well developed, mainly composed of three layers: (1) dorsal subcutaneous, located mainly close to the cutaneous musculature, with oblique fibres variously oriented (about 5–14 fibres thick); (2) supra-intestinal transverse (about 7–14 fibres thick); (3) subintestinal transverse (about 14–22 fibres thick). In addition, there are scattered transverse subneural fibres and ventral subcutaneous oblique fibres, as well as numerous dorso-ventral fibres. On the anterior region of the body (Figure 4A, B), the mesenchymal musculature is less developed than in the pre-pharyngeal region.

**Pharynx.** Pharynx cylindrical, about 5–6% of body length, with dorsal insertion posteriorly shifted, but located at the anterior third of pharyngeal pouch. Mouth posterior to the dorsal insertion, in the median third of pharyngeal pouch (Figure 4G).

Oesophagus short; oesophagus : pharynx ratio varying from 14% in paratype MZU PL.00190 to 18.5% in the holotype. It is lined by ciliated, cuboidal to columnar epithelium with some insunk nuclei. The oesophagus is coated with a thick subepithelial muscle layer with circular fibres, followed by a thin muscle layer with longitudinal fibres (about 60–100  $\mu$ m thick).

Pharynx and pharyngeal lumen lined by ciliated, cuboidal epithelium with insunk nuclei. Pharyngeal glands constituted by three secretory cell types: cells with fine granular erythrophil secretion; cells with fine granular xanthophil secretion and cells with amorphous cyanophil secretion. Cell bodies of pharyngeal glands located in the mesenchyme. Outer pharyngeal musculature (about 10–24  $\mu$ m thick) comprised of subepithelial layer of longitudinal muscles, followed by a circular layer and more

internally by longitudinal fibres. All layers become thinner towards pharyngeal tip and the longitudinal internal fibres become mixed with the circular fibres. Inner pharyngeal musculature (about 100–150  $\mu\text{m}$  thick) comprises a thick subepithelial layer with circular fibres, mixed internally and externally with longitudinal fibres. Inner musculature gradually becomes thinner towards pharyngeal tip.

**Reproductive organs.** Testes in one irregular row on either side of the body, located beneath the dorsal transverse mesenchymal muscles (Figure 4C, E). They begin slightly posterior to the ovaries, in the anterior third of the body, and extend to near the root of the pharynx (Table 1). Sperm ducts medial to ovovitelline ducts, above fibres of the subintestinal transverse mesenchymal musculature, in pre-pharyngeal region. They form spermiducal vesicles posterior to pharynx. Distally, spermiducal vesicles enter laterally into the proximal expanded portion of the prostatic vesicle (Figures 5A, B, 7A). Extrabulbar prostatic vesicle, unpaired, located near the common muscle coat, with ample proximal portion and tubular distal portion. The proximal portion is laterally expanded and T-shaped (Figures 5B, 7A); it is located closer to the ventral epidermis than to the dorsal epidermis. The prostatic vesicle penetrates the common muscle coat, becoming sinuous, and continues inside the penis papilla as an ejaculatory duct (Figure 5A). Ejaculatory duct slightly sinuous, opening through an expansion at the tip of the penis papilla (Figure 5B, 7B). Male atrium without folds, occupied by the conical and symmetric penis papilla with ventral insertion posteriorly displaced (Figures 5A, B, 6A, B, Table 1).

Lining epithelium of sperm ducts cuboidal and ciliated; thin muscularis (about 2–4  $\mu\text{m}$ ) constituted of interwoven circular and longitudinal fibres. Prostatic vesicle lined with ciliated, tall columnar or pseudostratified epithelium. Muscularis of prostatic vesicle (about 10–20  $\mu\text{m}$  thick) comprises circular fibres mixed with longitudinal and oblique fibres. Ejaculatory duct lined with ciliated, columnar epithelium, showing a pseudostratified appearance at the expanded portion (Figure 7B). Muscle coat of ejaculatory duct thin (about 3–5  $\mu\text{m}$ ), mainly constituted of circular fibres. Both prostatic vesicle and ejaculatory duct receive openings from glands producing a fine granular, mixed secretion (Figure 7A) as well as glands with amorphous cyanophil secretion. Granules with a mixed secretion have a cyanophil external part and an erythrophil internal core. Both glands with extrabulbar cell bodies.

Penis papilla lined with non-ciliated, pseudostratified epithelium. Penis glands produce numerous fine granular, xanthophil and erythrophil secretions as well as less numerous cyanophil secretions of two types (amorphous and fine granular secretion). All penis glands with cell bodies external to common muscle coat; their long necks run longitudinally through the papilla (Figures 6A, B, 7B), with numerous openings through its lining epithelium. Muscularis of the penis papilla (about 6–10  $\mu\text{m}$  thick) composed of a subepithelial circular layer, followed by a longitudinal layer.

Epithelial lining of male atrium columnar to pseudostratified (about 20–150  $\mu\text{m}$  thick), non-ciliated. Four types of glands empty through this epithelium: abundant cells with fine granular, cyanophil secretion and cells with cyanophil amorphous secretion; and few glands with fine granular, mixed secretion (cyanophil peripheral portion and erythrophil core) as well as scarce xanthophil glands. These glands have their cell bodies located in the mesenchyme, mainly anterior and laterally to the copulatory apparatus, or

between the fibres of the common muscle coat. Numerous necks of both types of cyanophil glands concentrate their openings at the dorso-lateral wall of the male atrium (Figure 6A, B). Their numerous gland necks are located between fibres of the stroma in the dorso-lateral walls of the male atrium. Muscularis of male atrium (about 4–8  $\mu\text{m}$  thick) comprised of a subepithelial layer with circular fibres, followed by a longitudinal layer.

Vitellaria (Figure 4C, F), situated between intestinal branches, opening into the ovovitelline ducts. Ovaries oval-elongate (Figure 4H), measuring about 300–520  $\mu\text{m}$  in diameter in the holotype and paratype MZU PL.00188, respectively. They are located dorsal to the ventral nerve plate, in the anterior third of the body (Table 1). Ovovitelline ducts emerge dorsally from the median third of the ovaries (Figure 4H) and run posteriorly immediately above the nerve plate. Lateral to the female atrium, ovovitelline ducts ascend postero-medially, to unite dorsal to the end of the median third or dorsal to the posterior third of the female atrium, thus forming the common glandular ovovitelline duct (Figures 5A, B, 6A). The female genital duct is dorso-anteriorly curved (Figures 5A, B, 6A). Female atrium, shorter than male atrium, funnel-shaped without folds (Figures 5A, B, 6A, B, Table 1).

Ovovitelline ducts and common ovovitelline duct lined with ciliated, cuboidal to columnar epithelium and covered with intermingled circular and longitudinal muscle fibres (about 3–5  $\mu\text{m}$ ). Numerous shell glands with erythrophil secretion empty into common glandular ovovitelline duct as well as into the distal half of the ascending portion of the ovovitelline ducts (Figures 5A, B, 6A, B).

Female genital duct and atrium lined by tall columnar to pseudostratified epithelium (Figure 6A) containing some lacunae. Female duct and atrium receive abundant cyanophil secretion of two types (amorphous and fine granular secretion), as well as erythrophil glands and few xanthophil glands. Their cell bodies are located between fibres of the atrial stroma or external to the common muscle coat. Muscularis of vagina and female atrium (about 15  $\mu\text{m}$  thick) composed mainly of circular fibres interposed with some longitudinal fibres.

Gonoduct vertical at the sagittal plane. Male and female atria with ample communication, without separating folds (Figures 5A, B, 6A, B). Gonoduct lined with ciliated columnar epithelium, receiving the openings of numerous rhabditogen glands and cyanophil glands with amorphous secretion. Muscularis of gonoduct comprised of a subepithelial layer of circular fibres, followed by a longitudinal layer.

Common muscle coat with circular, longitudinal and oblique fibres; it is thin along both male and female atria. A stroma with sparse intermingled muscle fibres separates the atrial muscularis and common muscle coat.

### **Variability**

Paratype MZU PL.000190 is at an initial stage of maturity, showing poorly developed testes and vitellaria, few shell glands and short female atrium. In paratype MZU PL.00187, the penis papilla is protruded towards the gonoduct and there is abundant cyanophil secretion in the male atrium and in the gonoduct; the epithelial lining of the female atrium is taller laterally than medially. The proximal portion of the prostatic vesicle contains sperm in paratype MZU PL.00189.

### Comparative discussion

In accordance with the phylogenetic analyses, the external and internal characters of the new species herein described as *Cratera ochra* sp. nov. strongly support its inclusion into the genus *Cratera* Carbayo et al. The morphological characters concern the following features: monolobated eyes, ejaculatory duct forming a distal cavity in the penis papilla and funnel-shaped female atrium.

*Cratera ochra* sp. nov., with dorsal eyes, can be differentiated from *Cratera pseudovaginuloides* (Riester, 1938), *Cratera yara* (E.M. Froehlich, 1955) and *Cratera cuarassu* Carbayo & Almeida, 2015, which have exclusively marginal eyes (E.M. Froehlich 1955; Froehlich 1956; Carbayo and Almeida 2015). It is also easily distinguished from *Cratera steffeni* Rossi et al., 2014, in which the eyes are restricted to either side of the body (Rossi et al. 2014). These four species and also *Cratera crioula* (E.M. Froehlich, 1955), *Cratera joia* (Froehlich, 1956) and *Cratera anamariae* Carbayo & Almeida, 2015 have different colour patterns in comparison to the new species herein described (Riester 1938; E.M. Froehlich 1955; Froehlich 1956; Rossi et al. 2014; Carbayo and Almeida 2015). *Cratera ochra* sp. nov. has colour and eye patterns similar to those of *Cratera tamoia* (E.M. Froehlich, 1955), but the new species can be mainly distinguished from the latter by its cylindrical pharynx, whereas the pharynx of *C. tamoia* is bell-shaped (E.M. Froehlich 1955).

With respect to the morphology of the copulatory apparatus, species of the genus *Cratera* have an extrabulbar prostatic vesicle, a penis papilla with a distal cavity and a funnel-shaped female atrium, among other characteristics. The prostatic vesicle has two portions, a proximal expanded section and a distal tubular and sinuous portion. In *C. ochra* sp. nov., similarly to *C. steffeni*, the proximal portion is characteristically T-shaped with the sperm ducts opening through its lateral walls. This form is particularly evident in horizontal sections of the copulatory apparatus. Other species of the genus, such as *C. crioula*, *C. joia*, *C. pseudovaginuloides* and *C. tamoia*, which were described as possessing a prostatic vesicle with proximal diverticula (Riester 1938; E.M. Froehlich 1955; Froehlich 1956), may have a vesicle with a similar form.

In summary, *C. ochra* sp. nov. is mainly differentiated from its congeners by the combination of the following morphological characters: dorsal body surface with dispersed pigmentation forming two broad bands, eyes spreading over the dorsal surface, cylindrical pharynx.

Measures of intraspecific and interspecific variation of the COI gene, as well as the ABGD algorithm applied to the COI data set, supported *C. ochra* sp. nov. as a species different from its congeners. In addition, both phylogenetic methods (maximum likelihood and Bayesian inference) revealed similar topologies, placing *C. ochra* sp. nov. as the sister group of the clade formed by *C. tamoia* and *C. crioula* (Figure 1).

### ***Obama maculipunctata* sp. nov.**

(Figures 8–11)

*Geoplana* sp. 5: Leal-Zanchet & Carbayo, 2000

*Geoplana* sp. 1: Carbayo et al., 2002

*Geoplana* sp. 2: Baptista et al., 2006

*Geoplana* sp. 2: Fick et al., 2006

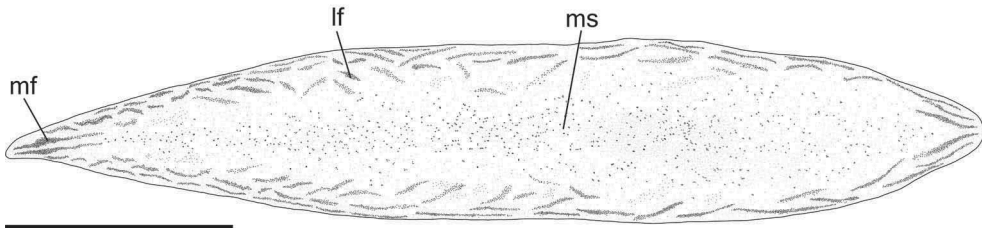
*Geoplana* sp. 3: Leal-Zanchet & Baptista, 2009

*Geoplana* sp. 3: Leal-Zanchet et al., 2011



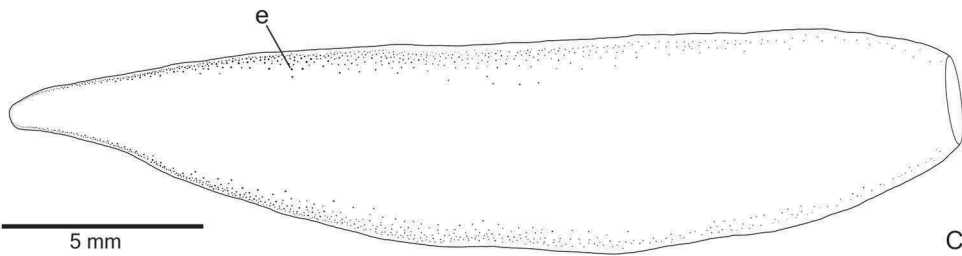
10 mm

A



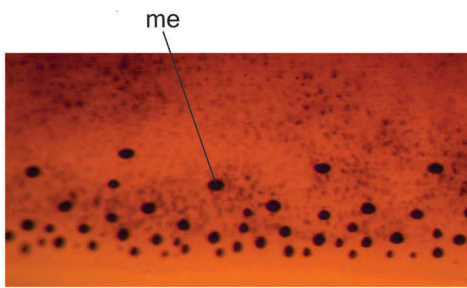
10 mm

B



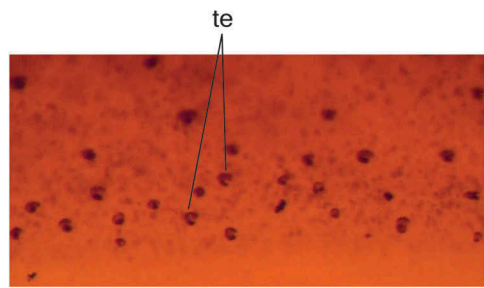
5 mm

C



0.5 mm

D



0.5 mm

E

**Figure 8.** *Obama maculipunctata* sp. nov. in dorsal view. (A) Photograph of a live specimen (holotype MZUSP PL.1565). (B) Dorsal pattern of pigmentation of the holotype. (C) Eye pattern of a fixed specimen (paratype MZU PL.00197). (D) Photograph of monolobated eyes of a fixed specimen (paratype MZU PL.00197) in clove oil. (E) Photograph of trilobated eyes of a fixed specimen (paratype MZU PL.00197) in clove oil.

### Etymology

The specific name refers to the dorsal pigmentation, which forms numerous flecks and dots.

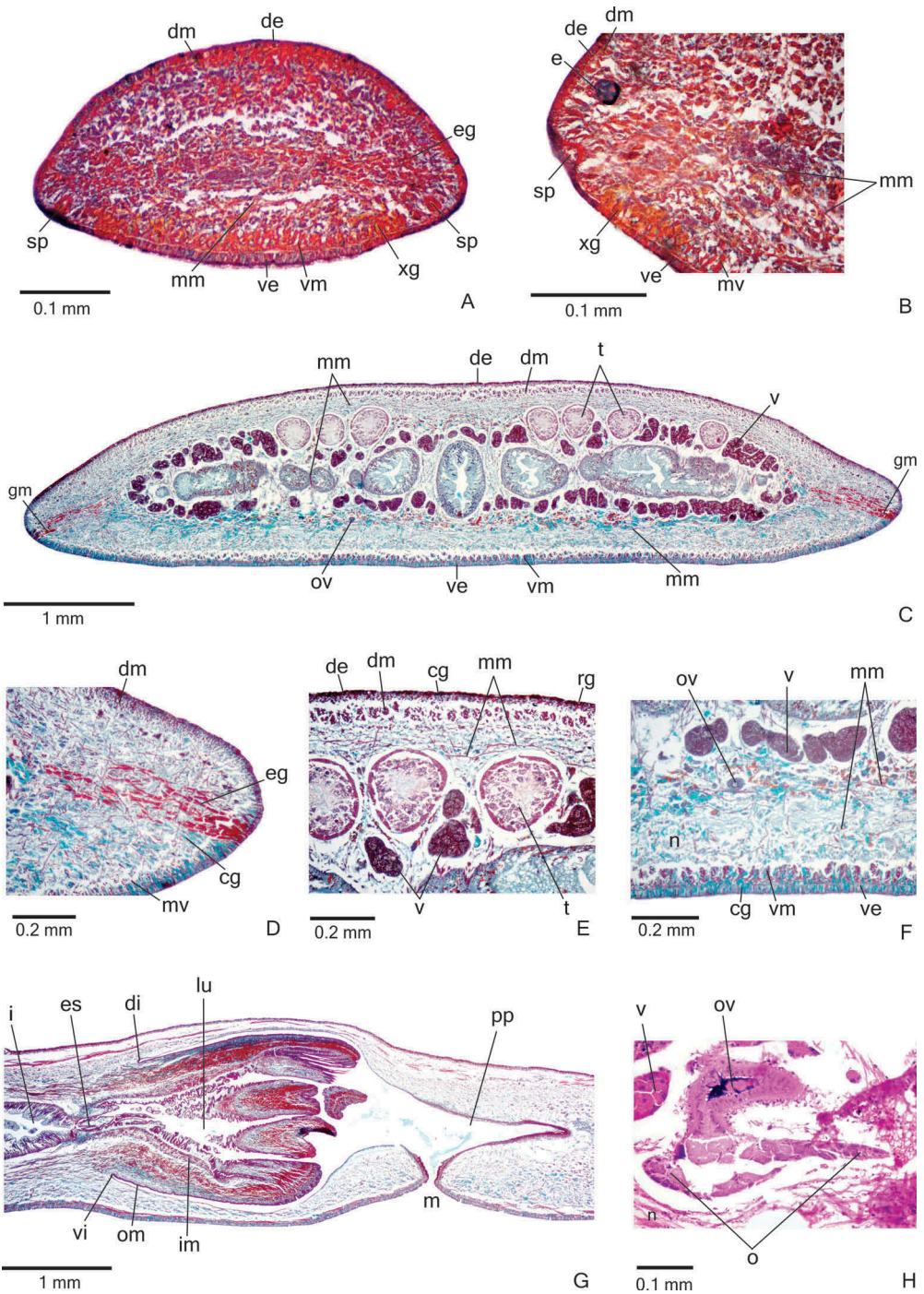


**Figure 9.** *Obama maculipunctata* sp. nov., holotype, in transverse (A–F) or sagittal (G, H) sections. (A) Anterior region of the body. (B) Detail of the anterior region of the body. (C) Pre-pharyngeal region. (D) Detail of body margin in the pre-pharyngeal region. (E) Detail of a dorsal portion of the pre-pharyngeal region. (F) Detail of a ventral portion of the pre-pharyngeal region. (G) Pharynx. (H) Ovary. In (H), the anterior portion of the ovary is not visible.

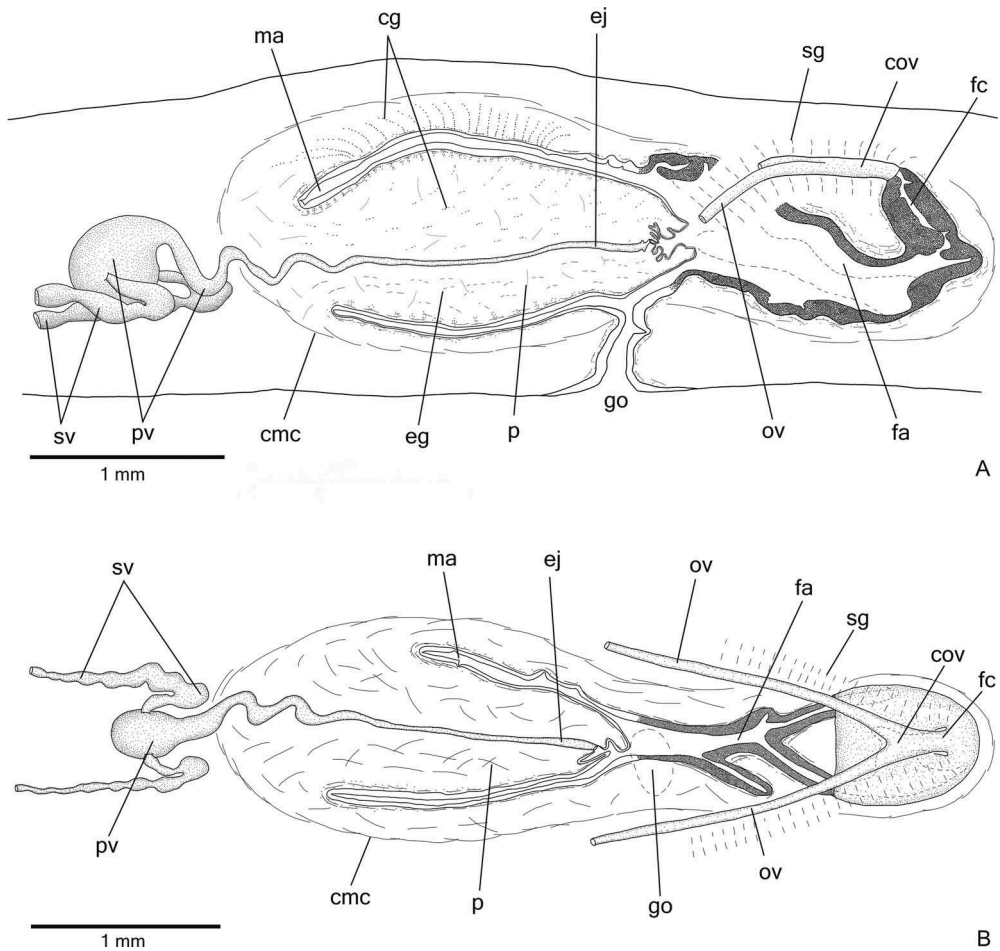


**Figure 10.** *Obama maculipunctata* sp. nov. (A) Sagittal composite reconstruction of the copulatory apparatus of the holotype. (B) Diagrammatic horizontal composite reconstruction of the copulatory apparatus of paratype MZU PL.00195.

### Type material

**Holotype.** MZUSP PL.1565: *leg.* P. K. Boll, 10 April 2014: São Francisco de Paula (National Forest of São Francisco de Paula), RS, Brazil – anterior tip: transverse sections on 21 slides; anterior region at the level of the ovaries: sagittal sections on 72 slides; pre-pharyngeal region: transverse sections on 20 slides; pharynx: sagittal sections on 36 slides; copulatory apparatus: sagittal sections on 40 slides.

**Paratypes.** MZU PL.00193: *leg.* R. Murowaniecki, 25 November 1997: São Francisco de Paula (National Forest of São Francisco de Paula), RS, Brazil – anterior tip: transverse sections on six slides; anterior region at the level of the ovaries: sagittal sections on 12 slides; pre-pharyngeal region: transverse sections on 11 slides; pharynx: sagittal sections on 42 slides; copulatory apparatus: sagittal sections on 36 slides. MZU PL.00194: *leg.* F. Carbayo, 11 December 1997: São Francisco de Paula (National Forest of São Francisco de

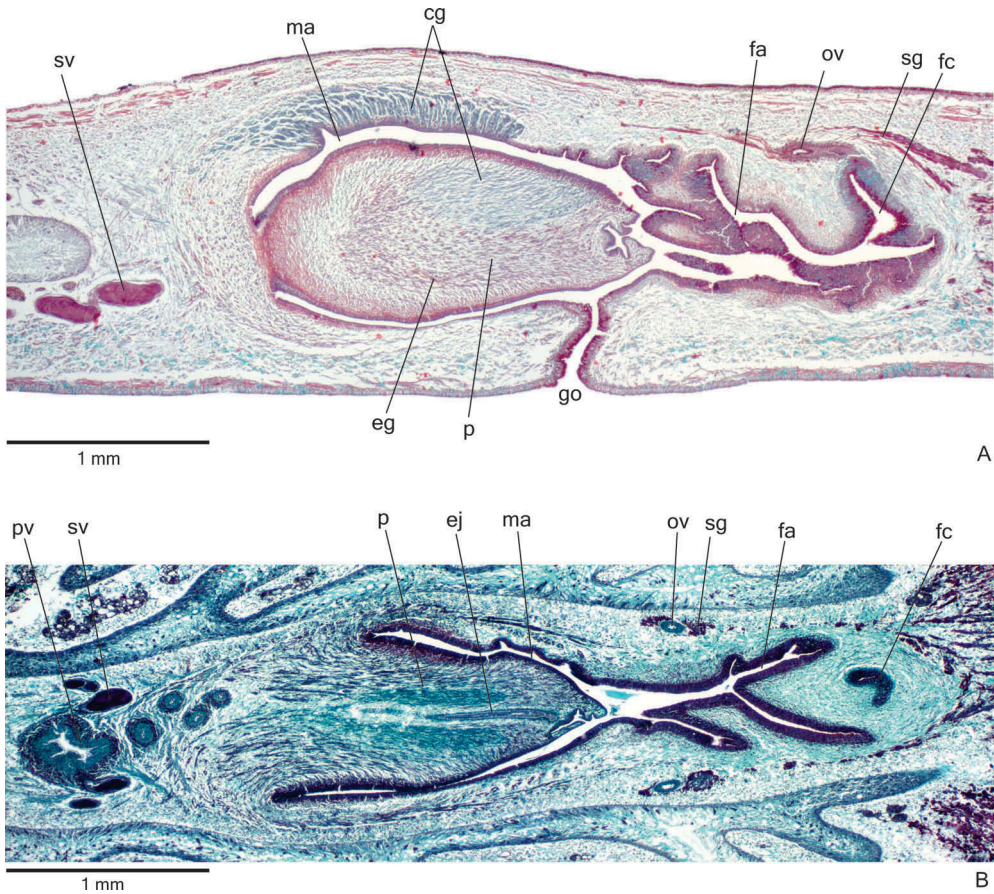


**Figure 11.** *Obama maculipunctata* sp. nov. (A) Copulatory apparatus of the holotype in sagittal section. (B) Copulatory apparatus of paratype MZU PL.00195 in horizontal section.

Paula), RS, Brazil – anterior tip: transverse sections on 18 slides; anterior region at the level of the ovaries: sagittal sections on 42 slides; pre-pharyngeal region: transverse sections on 15 slides; pharynx: sagittal sections on 29 slides; copulatory apparatus: sagittal sections on 34 slides. **MZU PL.00195:** *leg.* I. A. Fick, 25 November 1998: São Francisco de Paula (National Forest of São Francisco de Paula), RS, Brazil – pre-pharyngeal region: transverse sections on 12 slides; pharynx: sagittal sections on 36 slides; copulatory apparatus: horizontal sections on 34 slides. **MZU PL.00196:** *leg.* I. A. Fick, 23 June 2000: Praia Grande (National Park of Aparados da Serra), SC, Brazil – pre-pharyngeal region: transverse sections on 12 slides; pharynx: sagittal sections on 36 lâminas; copulatory apparatus: sagittal sections on 34 slides. **MZU PL.00197:** *leg.* S. V. Amaral, 21 March 2010: São Francisco de Paula (National Forest of São Francisco de Paula), RS, Brazil – anterior region preserved on clove oil; copulatory apparatus: sagittal sections on 27 slides.

#### **Type-locality**

National Forest of São Francisco de Paula, São Francisco de Paula, state of Rio Grande do Sul (RS), Brazil.

### **Distribution**

States of Rio Grande do Sul (São Francisco de Paula) and Santa Catarina (Praia Grande), Brazil.

### **Diagnosis**

Specimens of *Obama* with brown dorsum, sometimes greyish-brown, with a marbled appearance; live specimens with pale-yellow ventral surface in the anterior third and orange in the median and posterior thirds of the body; eyes spreading over the lateral parts of the dorsal surface; glandular margin with three types of glands; mc : h, 10–12%; pharynx cylindrical; prostatic vesicle with ovoid and unbranched proximal portion; penis papilla symmetrical and truncated with an almost straight ejaculatory duct; ovovitelline ducts emerging dorsally from the median third of ovaries and ascending anterior to the gonopore.

**Molecular diagnosis.** This species includes all populations that cluster with specimens KT250625 to KT250629 (see Supplementary material, Table S1), with significant support in phylogenetic analyses.

### **Description**

**External features.** Body lanceolate, elongate and flat; anterior end more narrowed than the posterior end (Figure 8A). When crawling, maximum length reaches 72 mm (Table 3). Mouth and gonopore located at the posterior third of the body, with the exception of the mouth in paratype MZU PL.00197, which is located at the median third of the body (Table 3).

Live specimens with brown dorsum, sometimes greyish-brown, with a marbled appearance (Figure 8A); ventral surface pale-yellow in the anterior third and orange in the median and posterior thirds of the body. Under moderate magnification, the anterior tip shows two median dark stripes, whereas the rest of the dorsum shows irregular greyish flecks laterally, over a light brown ground colour, and numerous dark-grey spots medially (Figure 8B). Under the stereomicroscope, dorsal ground-colour greyish, covered by fine brownish pigmentation with dark grey spots in a wide median zone of the body and flecks on the body margins. Flecks form two median stripes on the anterior and posterior tips; these stripes are more parallel to each other anteriorly (Figure 8B). In preserved specimens dorsal and ventral colour fade, the ventral surface becoming pale yellow.

Eyes, initially uniserial, surround anterior tip and become pluriserial immediately after this tip. After the fifth millimetre of the body, eyes spread over the lateral parts of the dorsum, forming a maximum of five longitudinal rows on either side of the dorsal surface (Figure 8C). They are monolobated, with pigment cups of about 30–60 µm in diameter, on the anterior third of the body (Figure 8D). After that, they are trilobated (with pigment cups of about 20–40 µm in diameter), occupying the lateral parts of the dorsal surface (Figure 8E), but become less numerous towards posterior tip. Clear halos around eyes are absent.

**Sensory organs, epidermis and body musculature.** Sensory pits (Figure 9A, B), as simple invaginations, contour anterior tip and occur ventromarginally in an irregular,

**Table 3.** Measurements, in mm, of specimens of *Obama maculipunctata* sp. nov.

	Holotype MZUSP PL.1565	Paratype MZU PL.00193	Paratype MZU PL.00194	Paratype MZU PL.00195	Paratype MZU PL.00196	Paratype MZU PL.00197
Maximum length in extension	65	66	60	72	42	–
Maximum width in extension	6	7	6	5	2.5	–
Length at rest	40	42	39	32	17	22
Width at rest	11	12	10	10	6	6
Length*	41	49	46	55	28.5	37
Width*	8	9	9	7	4.5	6
DM*	30 (73)	29.5 (60)	29 (63)	36 (65.5)	21 (73.5)	19 (51)
DG*	36 (88)	36 (73.5)	36 (78)	43 (78)	24 (84)	23 (62)
DMG*	6	6.5	7	7	3	–
DPVP	0.8	1.6	0.6	1.2	0.3	–
Ovaries	10 (24)	9.5 (19)	8 (17)	–	–	–
Anteriormost testes	12 (29)	10.5 (21.5)	8.5 (18.5)	–	–	–
Posteriormost testes	26 (63)	19 (39)	15 (33)	28.5 (52)	16 (56)	–
Prostatic vesicle	1	0.9	1	1.2	0.5	0.6
Penis papilla	2.3	2.3	1.4	1.5	1.5	1.8
Male atrium	2.6	1.7	1.6	1.5	0.8	1.1
Female atrium	1.6	2.8	1.8	2	1.4	1.1

–, not measured; \*, after fixation; DG, distance of gonopore from anterior end; DM, distance of mouth from anterior end; DMG, distance between mouth and gonopore; DPVP, distance between prostatic vesicle and pharyngeal pouch. The numbers given in parentheses represent the position relative to body length.

single row in the anterior seventh of the body. Initially they occur at intervals of approximately 12  $\mu\text{m}$ , becoming gradually sparser. Their depth is about 25–40  $\mu\text{m}$ .

Creeping sole occupying the whole body width. Three types of glands discharge through dorsal epidermis and body margins of the pre-pharyngeal region: numerous rhabditogen cells with xanthophil secretion (rhammites) and erythrophil cells with fine granular secretion, as well as few glands with amorphous, cyanophil secretion (Figure 9E). Creeping sole receives the secretion from numerous coarse granular, cyanophil glands (Figure 9F), as well as few rhabditogen glands with small, xanthophil rhabdites and cells with fine granular, erythrophil secretion. After the sixth millimetre of the body, glandular margin (Figure 9C, D) receiving openings of at least three types of glands: abundant glands with xanthophil, coarse granules, as well as scarcer erythrophil glands with fine granules and cyanophil glands with amorphous secretion. Some rhabditogen cells with small, xanthophil rhabdites open between cells of the glandular margin. On anterior tip (Figure 9A, B), glands with cyanophil secretion and scarce glands with fine granular, erythrophil secretion open through the whole surface of the body. In addition, numerous glands with coarse granular, xanthophil secretion open through the ventral epidermis and rhabditogen glands open through the dorsal epidermis and body margins.

Cutaneous musculature with the usual three layers (circular, oblique and longitudinal layers), longitudinal layer with thick bundles (Figure 9C–F, Table 4). Cutaneous musculature thinner in the pre-pharyngeal region than in the anterior region of the body, but gradually diminishing towards anterior tip. Musculature higher medially, becoming progressively lower towards body margins; ventral musculature higher than dorsal at the sagittal plane in the pre-pharyngeal region  $mc : h$  11–12% (Table 4).

**Table 4.** Body height and cutaneous musculature in the median region of a transverse section of the pre-pharyngeal region, in micrometers, and ratio of the height of cutaneous musculature to the height of the body (mc : h index) of specimens of *Obama maculipunctata* sp. nov.

	Holotype MZUSP PL.1565	Parratype MZU PL.00193	Paratype MZU PL.00194	Paratype MZU PL.00195
Dorsal musculature	85	75	69	70
Ventral musculature	65	81	88	90
Body height	1500	1581	1406	1300
mc : h (%)	10	10	11	12

Mesenchymal musculature (Figure 9C, E, F) mainly composed of three layers: (1) dorsal subcutaneous, located mainly close to the cutaneous musculature, with oblique fibres variously oriented (about three to four fibres thick); (2) supra-intestinal transverse (about 11–16 fibres thick); (3) subintestinal transverse (about seven to eight fibres thick). In addition, there are scattered ventral subcutaneous oblique fibres and transverse subneural fibres, as well as dorso-ventral fibres. On the anterior region of the body (Figure 9A, B), the mesenchymal musculature is less developed than in the pre-pharyngeal region.

**Pharynx.** Pharynx cylindrical with dorsal insertion shifted posteriorly, about 6–7% of the body length, occupying the first two-thirds of the pharyngeal pouch; mouth in the posterior third of pharyngeal pouch (Figure 9G). Oesophagus short; with folded wall. Oesophagus : pharynx ratio varying from 5% to 24% (10% in the holotype). It is lined by ciliated, cuboidal epithelium with insunk nuclei and coated with a thick muscle layer with circular fibres and various interposed longitudinal fibres (about 40–70  $\mu\text{m}$  thick).

Pharynx and pharyngeal lumen lined by ciliated, cuboidal epithelium with insunk nuclei. Pharyngeal glands constituted by three secretory cell types: abundant glands with fine granular erythrophil secretion; glands with fine granular xanthophil secretion; and glands with amorphous cyanophil secretion. Cell bodies of pharyngeal glands located in the mesenchyme, mainly anterior and posterior to the pharynx.

Outer pharyngeal musculature (about 20–30  $\mu\text{m}$  thick) comprised of thin subepithelial layer of longitudinal muscles, followed by a thicker layer of circular fibres. Inner pharyngeal musculature (about 50–110  $\mu\text{m}$  thick) comprises a thick subepithelial layer of circular fibres, interposed with various longitudinal fibres. Outer and inner musculatures gradually become thinner towards pharyngeal tip.

**Reproductive organs.** Testes in at least three irregular rows beneath the dorsal transverse mesenchymal muscles (Figure 9C, E). They begin in the anterior third of the body and extend to near the root of the pharynx (Table 3). Sperm ducts dorsal to ovovitelline ducts, in pre-pharyngeal region subdivided into three or four ductules. They form spermiducal vesicles posterior to the pharynx. Distally, spermiducal vesicles penetrate into the lateral wall of the proximal portion of the prostatic vesicle (Figures 10A, B, 11B). Prostatic vesicle extrabulbar, unpaired, and consisting of two portions: a globose proximal portion and a tubular, sinuous, distal portion (Figure 10A, B). The tubular portion penetrates the common muscle coat and continues inside the penis papilla as an ejaculatory duct. Ejaculatory duct almost straight, opening at the tip of a truncated penis papilla (Figures 10A, B, 11A, B). The

tip of the penis papilla may form a globose invagination with irregular contour (Figures 10A, 11A). Male atrium almost without folds, occupied by the conical and symmetrical penis papilla (Table 3, Figures 10A, B, 11A, B). The latter may occupy the distal part of the female atrium, as in paratypes MZU PL.00196 and MZU PL.00197.

Lining epithelium of sperm ducts cuboidal and ciliated; thin muscularis (about 6–10 µm thick) mainly constituted of circular fibres. Prostatic vesicle lined with ciliated, columnar or pseudostratified epithelium with irregular height. It receives abundant amorphous cyanophil secretions and scarcer fine granular erythrophil secretions, both from secretory cells with bodies lying in the mesenchyme, mainly around the vesicle. Muscularis of prostatic vesicle (about 50–120 µm thick) comprises interwoven longitudinal, oblique and circular fibres (Figure 11B). Ejaculatory duct lined with ciliated, columnar epithelium, receiving few openings from secretory cells with weakly cyanophil, amorphous secretion. Muscle coat of ejaculatory duct thin (about 10–20 µm thick), constituted of interwoven circular and longitudinal fibres.

Penis papilla covered with non-ciliated, columnar epithelium, becoming lower towards the tip of the papilla (Figure 11A, B). Penis glands of four types: cells with numerous fine granular erythrophil secretion, cells with mixed (cyanophil peripheral portion and erythrophil core), fine granular secretion and scarcer glands with cyanophil secretion and glands with xanthophil secretion. They run longitudinally in the papilla, with numerous openings through its covering epithelium, the erythrophil glands concentrating their openings at the tip and ventral surface of the penis papilla (Figure 11A). Penis glands with cell bodies mainly external to common muscle coat and among fibres of this coat. Muscularis of the penis papilla (about 30–60 µm thick) composed of a thick, subepithelial layer of circular fibres interposed with some longitudinal fibres.

Epithelial lining of male atrium columnar (about 10–25 µm thick), non-ciliated. Three types of secretory cells empty through this epithelium: glands with fine granular, erythrophil secretion, glands with amorphous cyanophil secretion and glands with fine granular mixed secretion (cyanophil peripheral portion and erythrophil core). Numerous necks of the latter concentrate their openings at the dorsal wall of the distal portion of the male atrium (Figure 11A). Muscularis of male atrium (about 15–45 µm thick) comprised of circular fibres and some interposed longitudinal fibres.

Vitellaria (Figure 9C, E, F), situated between intestinal branches, open into the ovovitelline ducts. Ovaries ovoid or oval-elongate (Figure 9H), measuring about 400 µm in diameter in the holotype and 200–300 µm in diameter in paratypes MZU PL.00194 and MZU PL.00193, respectively. They are dorsal to the ventral nerve plate, at the same transverse level as the anteriormost testes or slightly anterior to them. Ovovitelline ducts emerge dorsally (Figure 9H) from the median third of the ovaries and run posteriorly immediately above the nerve plate. Lateral to the female atrium, ovovitelline ducts ascend postero-medially, to unite dorsal to the median or posterior third of female atrium, so forming a short common glandular ovovitelline duct. Ental portion of female atrium with an antero-dorsally directed female canal (Figures 10A, B, 11A). Female atrium ovoid with folded walls (Figures 10A, B, 11A, B). Female atrium length about half that of male atrium in the holotype, but almost the same as male atrium length in most paratypes (Table 3).

Ovovitelline ducts and common oviduct lined with ciliated, cuboidal to columnar epithelium. They are covered with intermingled circular and longitudinal muscle fibres

(about 20–30 µm thick). Abundant shell glands with erythrophil secretion empty into the common glandular ovovitelline duct as well as in the distal half of the ascending portion of the ovovitelline ducts (Figures 10A, B, 11A, B).

Female atrium and canal lined by tall columnar epithelium, exhibiting a multilayered aspect in some places (Figure 11A) and with a xanthophil apical layer. Female atrium and canal receive abundant fine granular erythrophil secretion and cyanophil amorphous secretion. Cell bodies of both glands are located external to the common muscle coat or among its fibres. Muscularis of female atrium and canal (about 20–40 µm thick) composed of a subepithelial layer of interwoven circular and longitudinal fibres.

Gonoduct vertical at the sagittal plane. Male and female atria with ample communication, without separating folds (Figures 10A, B, 11A, B). Gonoduct lined with ciliated columnar epithelium, receiving the openings of abundant glands with fine granular erythrophil secretion and glands containing amorphous cyanophil secretion, as well as rhabditogen glands with small rhabdites. Muscularis of gonoduct consisting of a subepithelial layer of circular fibres, followed by a layer of longitudinal fibres.

Common muscle coat poorly developed, with circular, longitudinal and oblique fibres, thicker around male atrium than around female atrium. A stroma with sparse intermingled muscle fibres separates the atrial muscularis from the common muscle coat.

### Comparative discussion

In general, external and internal characteristics of *O. maculipunctata* sp. nov. match the diagnostic characteristics of the genus *Obama* Carbayo et al., 2013, so corroborating the molecular phylogenetic analyses. The new species of *Obama* herein described shows an internal morphology similar to four other species of this genus, namely *Obama fryi* (von Graff, 1899), *Obama polyophthalma* (von Graff 1899), *Obama carinata* (Riester, 1938) and *Obama eudoximariae* (Ogren & Kawakatsu, 1990). These species share an extrabulbar prostatic vesicle with a globose proximal portion, a symmetrical penis papilla with dorsal and ventral insertions at the same transverse level, and an ovoid female atrium (von Graff 1899; Schirch 1929; Riester 1938; Marcus 1951; Froehlich 1956; Ogren and Kawakatsu 1990).

Considering external features, by having a marbled colour pattern, the new species of *Obama* is similar to *O. polyophthalma*. It differs from *O. fryi*, *O. carinata* and *O. eudoximariae*, because they have homogeneous or striped patterns (von Graff 1899; Schirch 1929; Riester 1938; Marcus 1951; Froehlich 1956). Regarding the anatomy, *O. maculipunctata*, which has a cylindrical pharynx, can be differentiated from *O. carinata* and *O. eudoximariae* which have a collar-type pharynx (Schirch 1929; Riester 1938; Marcus 1951; Ogren and Kawakatsu 1990). In addition, *O. maculipunctata* differs from all four species by a combination of the following characteristics of the copulatory apparatus: unbranched proximal portion of the prostatic vesicle, truncated penis papilla, and almost straight ejaculatory duct traversing the penis papilla.

As a number of species of *Geoplana* incertae sedis have general characteristics similar to species of *Obama*, we have extended our comparative analysis of *O. maculipunctata* to this group of species. Among the 47 species indicated by Carbayo et al. (2013) as *Geoplana* incertae sedis, only one species, *Geoplana fuhrmanni* Hyman, 1962, from Panama, shows characteristics of the copulatory apparatus similar to those of *O. maculipunctata*. However, having a marbled dorsum, the new species can be

distinguished from *G. fuhrmanni*, with an almost homogeneous, spotted coloured dorsal surface, as well as by the morphology of the female atrium, which is short and funnel-shaped, in contrast to the large and ovoid female atrium of *O. maculipunctata*.

Comparison of the new species with its congeners, using measures of intraspecific and interspecific variation of the COI gene, as well as the ABGD tool applied to the COI data set, also supported *O. maculipunctata* sp. nov. as a separate species. Maximum likelihood and Bayesian inference phylogenies were congruent and indicated *O. maculipunctata* sp. nov. as the sister group of *O. carinata* (Figure 1).

### Notes on ecology and distribution

*Cratera ochra* sp. nov. has been recorded mainly inside and on the borders of sites with the native vegetation (mixed ombrophilous forest) of its type-locality (Leal-Zanchet and Carbayo 2000; Carbayo et al. 2002; Leal-Zanchet et al. 2011), with a low to moderate abundance. It was also recorded in an area of dense ombrophilous forest, but not in areas of mixed ombrophilous forest, of the Research and Conservation Center Pró-Mata (Leal-Zanchet et al. 2011). *Obama maculipunctata* sp. nov. is abundant in areas of mixed ombrophilous forest of the Araucaria Plateau, as well as in plantations of the native *Araucaria angustifolia* and *Pinus* spp. of its type-locality (Leal-Zanchet and Carbayo 2000; Carbayo et al. 2002). It was also recorded in areas of mixed and dense ombrophilous forest of the Aparados da Serra National Park (Baptista et al. 2006; Fick et al. 2006), but it was not recorded in the Research and Conservation Center Pró-Mata (Leal-Zanchet et al. 2011).

### General discussion

In general, the two new species herein described match the diagnostic characteristics of their respective genera, despite their gross similarities. Species of *Cratera* and *Obama* have a similar external morphology, with a lanceolate body, usually slightly more leaf-shaped in species of *Obama* than in species of *Cratera*. Species of *Obama* can be distinguished from *Cratera*, as well as from other genera split off from *Geoplana*, by having trilobated eyes in addition to monolobated eyes (Carbayo et al. 2013). Other anatomical features, such as the distribution pattern of the sensory pits and details of the copulatory apparatus are useful in the identification of the species. Some of these features are noteworthy especially the distribution pattern of the sensory pits and the morphology of the prostatic vesicle.

In relation to the distribution pattern of the sensory pits in both genera, Carbayo et al. (2013) indicated that members of *Cratera* have the sensory pits arranged in a single row on either side of the body, whereas members of *Obama* have two to four rows of sensory pits on either side. However, we have observed that a single irregular longitudinal row of sensory pits on either side of the body is present in *O. maculipunctata*. As this character may be important for distinguishing monophyletic groups, it should be further investigated in other species of *Obama*.

Another feature that should be analysed in more detail in species of *Obama* is the morphology of the prostatic vesicle. Various species have an anteriorly branched prostatic vesicle, but this feature may not have been properly assessed in earlier descriptions (cf. von Graff 1899; Schirch 1929; Riester 1938; Marcus 1951). In *O. maculipunctata*, the proximal portion of the prostatic vesicle is clearly unbranched.

The genus *Cratera*, with eight formally described species (Carbayo et al. 2013; Rossi et al. 2014; Carbayo and Almeida 2015), had the type-species and four others molecularly analysed (Carbayo et al. 2013). In contrast, the genus *Obama*, originally with 34 species, was poorly investigated at the molecular level. Four species of *Obama* were analysed by Carbayo et al. (2013) and, more recently, two new species were proposed for the genus based on morphological and molecular studies (Álvares-Presas et al. 2015). It is noteworthy that one of the species included in the present phylogenetic analysis, *O. carinata*, showed a high intraspecific distance in relation to other species of the group. These results are also supported by the ABGD analysis, which split the specimens of *O. carinata* into two major mitochondrial DNA lineages, suggesting that they are two potential species. However, a Bayesian phylogenetics and phylogeography analysis (Yang and Rannala 2010) applied for a large data set indicated that the specimens of *O. carinata* constituted a single species (Álvares-Presas et al. 2015). In fact, Puillandre et al. (2012) point out that the partition output by ABGD should be considered as a first species partition hypothesis, since this result arises from the evaluation of pairwise differences of a single molecular marker. Therefore, the definition of the taxonomic status should be complemented with other evidence, such as morphological data, as done herein, in an integrative taxonomic approach (Will et al. 2005; Padial et al. 2009; Puillandre et al. 2012).

## Acknowledgements

We gratefully acknowledge the Conselho Nacional de Desenvolvimento Científico e Tecnológico (CNPq), the Coordenação de Aperfeiçoamento de Pessoal de Nível Superior (CAPES) and the Fundação de Amparo à Pesquisa do Rio Grande do Sul (FAPERGS) for research grants and fellowships in support of this study. We acknowledge C.M. Palácios, F. Carbayo, P.K. Boll and R. Murowaniecki, for their help in sampling flatworms. P.K. Boll is thanked for photographs of the live specimen of *Cratera ochra*. We are grateful to two anonymous reviewers for their valuable suggestions on an early draft of the paper. We acknowledge Prof. Dr. Eudóxia Froehlich (im memoriam) for the openness in sharing her profound knowledge on land flatworms with us over many years of a deep friendship.

## Disclosure statement

No potential conflict of interest was reported by the authors.

## ORCID

Ana Maria Leal-Zanchet  <http://orcid.org/0000-0003-3927-5629>

## References

- Álvares-Presas M, Amaral SV, Carbayo F, Leal-Zanchet AM, Riutort M. 2015. Focus on the details: morphological evidence supports new cryptic land flatworm (Platyhelminthes) species revealed with molecules. *Org Divers Evol*. doi:10.1007/s13127-014-0197-z
- Álvarez-Presas M, Carbayo F, Rozas J, Riutort M. 2011. Land planarians (Platyhelminthes) as a model organism for fine-scale phylogeographic studies: understanding patterns of biodiversity in the Brazilian Atlantic Forest hotspot. *J Evol Biol*. 24:887–896.

- Amaral SV, Oliveira SM, Leal-Zanchet AM. 2012. Three new species of land flatworms and comments on a complex of species in the genus *Geoplana* Stimpson (Platyhelminthes: Continenticola). *Zootaxa*. 3338:1–32.
- Baptista VA, Matos LB, Fick IA, Leal-Zanchet AM. 2006. Composição de comunidades de planárias terrestres (Platyhelminthes, Tricladida, Terricola) do Parque Nacional dos Aparados da Serra, Brasil. *Iheringia*. 96:293–297. doi:[10.1590/S0073-47212006000300004](https://doi.org/10.1590/S0073-47212006000300004)
- Carbayo F. 2010. A new genus for seven Brazilian land planarian species split off from *Notogynaphallia* (Platyhelminthes, Tricladida). *Belg J Zool*. 140:91–101.
- Carbayo F, Almeida AL. 2015. Anatomical deviation of male organs of land planarians from Rio de Janeiro, Brazil, with description of two new species of *Cratera* (Platyhelminthes, Tricladida). *Zootaxa*. 3931:27–40.
- Carbayo F, Álvarez-Presas M, Olivares CT, Marques FPL, Froehlich EM, Riutort M. 2013. Molecular phylogeny of Geoplaninae (Platyhelminthes) challenges current classification: proposal of taxonomic actions. *Zool Scr*. 42:508–528.
- Carbayo F, Froehlich EM. 2008. Estado do conhecimento dos macroturbelários (Platyhelminthes) do Brasil. *Biota Neotrop*. 8:177–197.
- Carbayo F, Leal-Zanchet AM, Vieira EM. 2002. Terrestrial flatworm (Platyhelminthes: Tricladida: Terricola) diversity versus man-induced disturbance in ombrophilous forest in Southern Brazil. *Biodivers Conserv*. 11:1091–1104.
- Carranza S, Littlewood DTJ, Clough KA, Ruiz-Trillo I, Baguña J, Riutort M. 1998. A robust molecular phylogeny of the Tricladida (Platyhelminthes: Seriata) with a discussion on morphological synapomorphies. *Proc Roy Soc Lond B*. 265:631–640.
- Fick IA, Leal-Zanchet AM, Vieira EM. 2006. Community structure of land flatworms (Platyhelminthes, Terricola): comparisons between Araucaria and Atlantic forest in Southern Brazil. *Inv Biol*. 125:306–313. doi:[10.1111/j.1744-7410.2006.00062.x](https://doi.org/10.1111/j.1744-7410.2006.00062.x)
- Froehlich CG. 1955. Sobre morfologia e taxonomia das Geoplanidae. *Bol Fac Fil Ci Letr Zoologia*. 19:195–279.
- Froehlich EM. 1955. Sobre espécies brasileiras do gênero *Geoplana*. *Bol Fac Fil Ci Letr Zoologia*. 19:289–369.
- Froehlich CG. 1956. Planárias terrestres do Paraná. *Dusenica*. 7:173–191.
- Grau JH, Sluys R, Froehlich EM, Carbayo F. 2012. Reflections on the genus *Amaga* Ogren and Kawakatsu 1990, and description of a new genus of land planarian (Platyhelminthes, Tricladida, Geoplanidae). *J Nat Hist*. 46:1529–1546.
- Hall TA. 1999. BioEdit: a user-friendly biological sequences alignment editor and analysis program for Windows 95/98 NT. *Nucleic Acids Symp Ser*. 41:95–98.
- Hyman LH. 1962. Some land planarians from Caribbean countries. *Am Mus Novitates*. 2110:1–25.
- IBGE. 1986. Levantamento de Recursos Naturais. Rio de Janeiro: SEPLAN/ Fundação Instituto Brasileiro de Geografia e Estatística – IBGE.
- Jones HD, Webster BL, Littlewood DTJ, McDonald JC. 2008. Molecular and morphological evidence for two new species of terrestrial planarians of the genus *Microplana* (Platyhelminthes; Turbellaria; Tricladida; Terricola) from Europe. *Zootaxa*. 1945:1–38.
- Kimura M. 1980. A simple method for estimating evolutionary rates of base substitutions through comparative studies of nucleotide sequences. *J Mol Evol*. 16:111–120.
- Lang A. 1884. Die Polycladen (Seeplanarien) des Golfes von Neapel und der angrenzenden Meeresabschnitte. Eine Monographie. Fauna Flora Golfes Neapel. Leipzig: Engelmann.
- Lázaro EM, Sluys R, Pala M, Stocchino GA, Baguña J, Riutort M. 2009. Molecular barcoding and phylogeography of sexual and asexual freshwater planarians of the genus *Dugesia* in the Western Mediterranean (Platyhelminthes, Tricladida, DugesIIDae). *Mol Phyl Evol*. 52:835–845.
- Leal-Zanchet AM, Baptista VA. 2009. Floresta com Araucária: Ecologia, Conservação e Desenvolvimento Sustentável. Ribeirão Preto: Holos. Chapter 19, Planárias terrestres (Platyhelminthes, Tricladida) em remanescentes de Floresta com Araucária; p. 199–207.
- Leal-Zanchet AM, Baptista VA, Campos LM, Raffo JF. 2011. Spatial and temporal patterns of land flatworm assemblages in Brazilian Araucaria forests. *Inv Biol*. 130:25–33.

- Leal-Zanchet AM, Carbayo F. 2000. Fauna de planárias terrestres (Platyhelminthes, Tricladida, Terricola) da Floresta Nacional de São Francisco de Paula, RS, Brasil: Uma análise preliminar. *Acta Biol Leopold.* 22:19–25.
- Lemos VS, Cauduro GP, Valiati VH, Leal-Zanchet AM. 2014. Phylogenetic relationships within the flatworm genus *Choeradoplana* Graff (Platyhelminthes: Tricladida) inferred from molecular data with the description of two new sympatric species from *Araucaria* moist forests. *Invertebr Syst.* 28:605–627.
- Marcus E. 1951. Sobre Turbellaria Brasileiros. *Bol Fac Fil Ci Letr Zoologia.* 16:5–215.
- Mateos E, Giribet G, Carranza S. 1998. Terrestrial planarians (Platyhelminthes, Tricladida, Terricola) from the Iberian Peninsula: first records on the family Rhynchodemidae with the description of a new *Microplana* species. *Contrib Zool.* 67:267–276.
- Nimer E. 1989. *Climatologia do Brasil.* Rio de Janeiro: Fundação Instituto Brasileiro de Geografia e Estatística.
- Ogren RE, Kawakatsu M. 1990. Index to the species of the family Geoplanidae (Turbellaria, Tricladida, Terricola). Part I: Geoplaninae. *Bull. Fuji Women's Coll.* 28:79–166.
- Padial JM, Castroviejo-Fisher S, Köhler J, Vilà C, Chaparro JC, De la Riva I. 2009. Deciphering the products of evolution at the species level: the need for an integrative taxonomy. *Zool Scripta.* 38:431–447.
- Posada D, Crandall KA. 1998. A modeltest: testing the model of DNA substitution. *Bioinformatics.* 14:817–818.
- Puillandre N, Lambert A, Brouillet S, Achaz G. 2012. ABGD, Automatic Barcode Gap Discovery for primary species delimitation. *Mol Ecol.* 21:1864–1877.
- Riester A. 1938. Beiträge zur Geoplaniden-Fauna Brasiliens. *Abh Senckenberg Naturf Ges.* 441:1–88.
- Romeis B. 1989. *Mikroskopische Technik.* München: Urban und Schwarzenberg.
- Ronquist F, Huelsenbeck JP. 2003. MrBayes 3: Bayesian phylogenetic inference under mixed models. *Bioinformatics.* 19:1572–1574.
- Rossi I, Fontoura M, Amaral S, Leal-Zanchet AM. 2014. A new species of land flatworm (Platyhelminthes: Continenticola) from areas of *Araucaria* Forest in southern Brazil. *Zootaxa.* 3794:514–524.
- Schirch PF. 1929. Sobre as planárias terrestres do Brasil. *Bol Mus Nacional.* 5:27–38.
- Sluys R, Kawakatsu M, Riutort M, Bagnà J. 2009. A new higher classification of planarian flatworms (Platyhelminthes, Tricladida). *J Nat Hist.* 43:1763–1777.
- Stamatakis A, Hoover P, Rougemont J. 2008. A rapid bootstrap algorithm for the RAxML Web servers. *Syst Biol.* 57:758–771.
- Stimpson W. 1857. *Prodromus descriptionis animalium evertibratorum, quae in Expeditione ad Oceanum Pacificum Septentrionalem a Republica Federata missa, Johanne Rodgers Duce, observavit et descripsit.* Pars I, Turbellaria Dendrocoela. *Proc Acad Sci Philadelphia.* 9:19–31.
- Sunnucks P, Blacket MJ, Taylor JM, Sands CJ, Ciavaglia SA, Garrick RC, Tait NN, Rowell DM, Pavlova A. 2006. A tale of two flatties: different responses of two terrestrial flatworms to past environmental climatic fluctuations at Tallaganda in montane southeastern Australia. *Mol Ecol.* 15:4513–4531.
- Swofford DL. 1998. *PAUP\*: phylogenetic analysis using parsimony (and other methods).* Sunderland, MA: Sinauer Associates.
- Tamura K, Peterson D, Peterson N, Stecher G, Nei M, Kumar S. 2011. MEGA5: molecular evolutionary genetics analysis using maximum likelihood, evolutionary distance and maximum parsimony methods. *Mol Biol Evol.* 28:2731–2739.
- Thompson JD, Gibson TJ, Plewniak F, Jeanmougin F, Higgins DG. 1997. The CLUSTAL\_X windows interface: flexible strategies for multiple sequence alignment aided by quality analysis tools. *Nucleic Acids Res.* 25:4876–4882.
- von Graff L. 1899. *Monographie der Turbellarien: II. Tricladida Terricola.* Leipzig: Engelmann.
- Will KW, Mishler BD, Wheeler QD. 2005. The perils of DNA barcoding and the need for integrative taxonomy. *Syst Biol.* 54:844–851.
- Yang Z, Rannala B. 2010. Bayesian species delimitation using multilocus sequence data. *Proc Natl Acad Sci USA.* 107:9264–9269.